Chapter 3

The Effects of Ground

The ground around and under an antenna is part of the environment in which any actual antenna must operate. Chapter 2, Antenna Fundamentals, dealt mainly with theoretical antennas in free space, completely removed from the influence of the ground. This chapter is devoted to exploring the interactions between antennas and the ground.

The interactions can be analyzed depending on where they occur relative to two areas surrounding the antenna: the *reactive near field* and the *radiating far field*. You will recall that the reactive near field only exists very close to the antenna itself. In this region the antenna acts as though it were a large lumped-constant inductor or capacitor, where energy is stored but very little is actually radiated. The interaction with the ground in this area creates mutual impedances between the antenna and its environment and these interactions not only modify the feed-point impedance of an antenna, but also often increase losses.

In the radiating far field, the presence of ground profoundly influences the radiation pattern of a real antenna. The interaction is different, depending on the antenna's polarization with respect to the ground. For horizontally polarized antennas, the *shape* of the radiated pattern in the elevation plane depends primarily on the antenna's height above ground. For vertically polarized antennas, both the *shape* and the *strength* of the radiated pattern in the elevation plane strongly depend on the nature of the ground itself (its dielectric constant and conductivity at the frequency of operation), as well as on the height of the antenna above ground.

The Effects of Ground in the Reactive Near Field

FEED-POINT IMPEDANCE VERSUS HEIGHT ABOVE GROUND

Waves radiated from the antenna directly downward reflect vertically from the ground and, in passing the antenna on their upward journey, induce a voltage in it. The magnitude and phase of the current resulting from this induced voltage depends on the height of the antenna above the reflecting surface.

The total current in the antenna consists of two components. The amplitude of the first is determined by the power supplied by the transmitter and the free-space feed-point resistance of the antenna. The second component is induced in the antenna by the wave reflected from the ground. This second component of current, while considerably smaller than the first at most useful antenna heights, is by no means insignificant. At some heights, the two components will be in phase, so the total current is larger than is indicated by the free-space feed-point resistance. At other heights, the two components are out of phase, and the total current is the difference between the two components.

Changing the height of the antenna above ground will change the amount of current flow, assuming that the power input to the antenna is constant. A higher current at the same power input means that the effective resistance of the

antenna is lower, and vice versa. In other words, the feedpoint resistance of the antenna is affected by the height of the antenna above ground because of mutual coupling between the antenna and the ground beneath it.

The electrical characteristics of the ground affect both the amplitude and the phase of reflected signals. For this reason, the electrical characteristics of the ground under the antenna will have some effect on the impedance of that antenna, the reflected wave having been influenced by the ground. Different impedance values may be encountered when an antenna is erected at identical heights but over different types of earth.

Fig 1 shows the way in which the radiation resistance of horizontal and vertical half-wave antennas varies with height above ground (in λ, wavelengths). The height of the vertical half-wave is the distance from the bottom of the antenna to ground. For horizontally polarized half-wave antennas, the differences between the effects of perfect ground and real earth are negligible if the antenna height is greater than 0.2 λ. At lower heights, the feed-point resistance over perfect ground decreases rapidly as the antenna is brought closer to a theoretically perfect ground, but this does not occur so rapidly for actual ground. Over real earth, the resistance actually begins increasing at heights below about 0.08 λ. The reason for the increasing resistance at very low heights is that more and more of the reactive (induction) field of the antenna is absorbed by the lossy ground in close proximity. This results in increased loss that is reflected in the increased value of the feedpoint resistance.

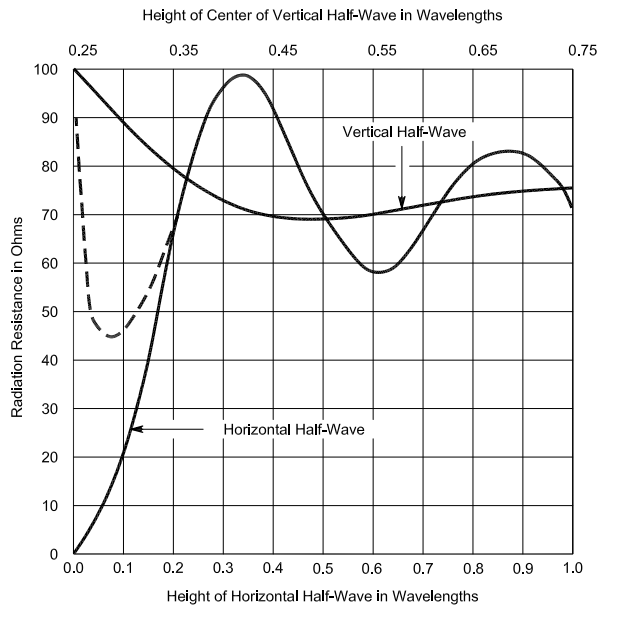

Fig 1—Variation in radiation resistance of vertical and horizontal half-wave antennas at various heights above flat ground. Solid lines are for perfectly conducting ground; the broken line is the radiation resistance of horizontal half-wave antennas at low height over real ground.

For a vertically polarized λ/2-long dipole, differences between the effects of perfect ground and real earth on the feed-point impedance is negligible, as seen in **Fig 1**. The theoretical half-wave antennas on which this chart is based are assumed to have infinitely thin conductors.

GROUND SYSTEMS FOR VERTICAL MONOPOLES

In this section, we'll look at vertical monopoles, which require some sort of ground system in order to make up for the "missing" second half of the antenna and reduce the power lost in the near field. Rudy Severns, N6LF, contributed much of the new material in this chapter.

In Chapter 2, Antenna Fundamentals, and up to this point in this chapter, the discussion about vertical monopoles has mainly been for antennas where *perfect ground* is available. We have also briefly looked at the ground-plane vertical in free space, where the four ground-plane radials form a built-in ground system.

Perfect ground makes a vertical monopole into the functional equivalent of a center-fed dipole, although the feedpoint resistance at resonance is half that of the center-fed dipole. But how can we manage to create that elusive perfect ground, or at least a reasonable approximation, for our real vertical antennas?

Simulating a Perfect Ground in the Reactive Near Field

The effect of a perfectly conducting ground (so far as feed-point resistance and losses are concerned) can be simulated under a real antenna by installing a very large metal screen or mesh, such as poultry netting (chicken wire) or hardware cloth, on or near the surface of the ground. The screen (also called a *counterpoise system*, especially if it is elevated off the ground) should extend at least a half wavelength in every direction from the antenna. The feed-point resistance of a quarter-wave long, thin vertical radiator over such a ground screen will approach the theoretical value of 36.6 Ω. Of course on the lower HF bands such a screen is not practical for most amateurs.

Based on the results of a study published in 1937 by Brown, Lewis and Epstein (see Bibliography), a grounding system consisting of 120 wires, each at least λ/2 long, extending radially from the base of the antenna and spaced equally around a circle, is also the practical equivalent of perfectly conducting ground for reactive-field currents. The wires can either be laid directly on the surface of the ground or buried a few inches below.

Another approach to simulating a perfect ground system is to utilize the ground-plane antenna, with its four ground-plane radials elevated well above lossy earth. Heights (between the bottom of the ground-plane and the surface of the ground) greater than λ/8 have proven to yield excellent

results. See Chapter 6, Low-Frequency Antennas, for more details on practical ground-plane verticals.

For a vertical antenna, a large ground screen, either made of wire mesh or a multitude of radials, or an elevated system of ground-plane radials will reduce ground losses near the antenna. This is because the screen conductors are solidly bonded to each other and the resistance is much lower than that of the lossy, low-conductivity earth itself. If the ground screen or elevated ground plane were not present, RF currents would be forced to flow through the lossy, low-conductivity earth to return to the base of the radiator. The ground screen or elevated ground plane in effect shield ground-return currents from the lossy earth.

Less-Than-Ideal Ground Systems

Now, what happens when something less than an ideal ground screen is used as the ground plane for a vertical monopole? Typically this will take the form of an on-ground wire radial system. A great deal of mystery and lack of information seems to surround the vertical antenna ground system. In the case of ground-mounted vertical antennas, many general statements such as "the more radials the better" and "lots of short radials are better than a few long ones" have served as rules of thumb, but many questions as to relative performance differences and optimum number for a given length remain unanswered, as is the justification for the rules of thumb. Most of these questions boil down to one: namely, how many radials, and how long, should be used in a given vertical antenna installation?

A ground system with 120 $\lambda/2$ radials is not very practical for many amateur installations, which often must contend with limited space and funding. Unfortunately the ground resistance, R_g, increases rapidly when the number of radials is reduced. To minimize ground loss where a large, optimum ground system is not possible requires that we understand how ground losses occur and how to optimize the design of a ground system that can fit within the space and budget available.

E and H Fields

E and H fields were introduced in Chapter 2, Antenna Fundamentals, to explain some basic concepts concerning antennas. To understand the reasons for ground loss we need to look at the E and H fields in the near field, but we need to have some feeling for what E and H fields are. The following is a brief description of these fields. It is certainly not a rigorous description but should give at least an intuitive feeling for what is happening.

In 1820 Hans Oerstad discovered that a current flowing in a wire would deflect the needle of a nearby compass. We attribute this effect to a *magnetic* or *H-field*, which at any given location is denoted by the bold-faced letter **H**. **H** is a vector, with an amplitude expressed in A/m (Amperes/meter) and a direction. **Fig 2** shows a typical experimental arrangement. The shape of the magnetic field is roughly shown by the distribution of the iron filings. This field distribution is very similar to that for a vertical antenna.

A compass needle (a small magnet itself) will try to align itself parallel to **H.** As the compass is moved around the conductor, the orientation of the needle changes accordingly. The orientation of the needle gives the direction of **H**. If you attempt to turn the needle away from alignment you will discover a torque trying to restore the needle to its original position. The torque is proportional to the strength of the magnetic field at that point. This is called the *field intensity* or amplitude of **H** at that point. If a larger current flows in the conductor going through the piece of paper holding the iron filings, the amplitude of **H** will be larger. Currents flowing in the conductors of an antenna also generate a magnetic field, one component of the near field.

An antenna will also have an *electric* or *E-field*, which can be visualized using a parallel-plate capacitor, as shown in **Fig 3**. If we connect a battery with a potential V_{dc} across the capacitor plates there will be an electric field **E** established between the plates, as indicated by the lines and directional arrows between the plates. The magnitude of vector **E** is expressed in V/m (volts per meter), so for a potential of V volts and a spacing of d meters, E = V/d V/m. The amplitude of **E** will increase with greater voltage and/or a smaller distance (d). In an antenna, there will be ac potential differences between different parts of the antenna and from the antenna to ground. These ac potential differences establish the electric field associated with the antenna.

Conduction And Displacement Currents

If we replace the dc voltage source in Fig 3 with an ac source, a steady ac current will flow in the circuit. In the

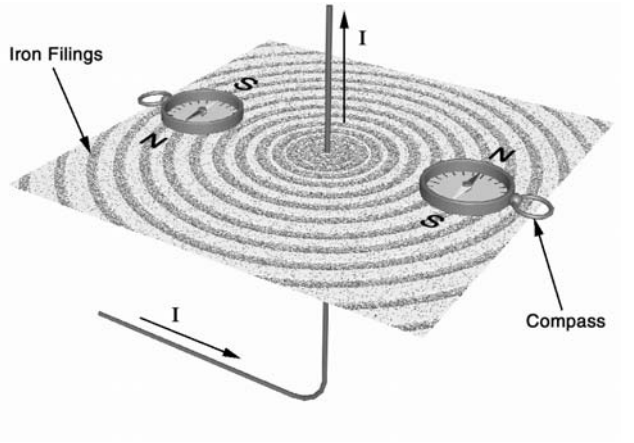

Fig 2—The magnetic lines of force that surround a conductor with an electric current flowing in it are shown by iron filings and small compass needles. The needles point in the direction of the magnetic or H-field. The filings give a general view of the field distribution in the plane perpendicular to the conductor.

conductors between the ac source and the capacitor plates, current (I_c) flows, because of the movement of charge, usually electrons. But in the space between the capacitor plates—particularly in a vacuum—there are no charge carriers available to carry a conduction current. Nonetheless, current still flows in the complete circuit, and we attribute this to a *displacement current* (I_d) flowing between the capacitor plates to account for the continuity of current in the circuit. Displacement and conduction currents are two different phenomena but they both represent current, just two different kinds. Some observers prefer to call conduction currents "currents" and displacement currents "imaginary currents." That terminology is OK, but to account for the current flow in a closed circuit with capacitance you have to keep track of both kinds of current, whatever you call them.

In an antenna over ground, the displacement current represents the current flow from the antenna surface through the air into the ground. The currents flowing in the ground are predominantly conduction currents, but there may also be displacement currents.

Where the dielectric material between the capacitor plates is not a perfect insulator, both conduction and displacement currents can flow between the capacitor plates. A good example of this would be a soil dielectric, which has both resistive and capacitive characteristics. Soil can be represented in the circuit of **Fig 4**, where there is a resistor with a conduction current I_c in parallel with a capacitor with a displacement current I_d. The two currents add up (vectorially) as the total current I_T.

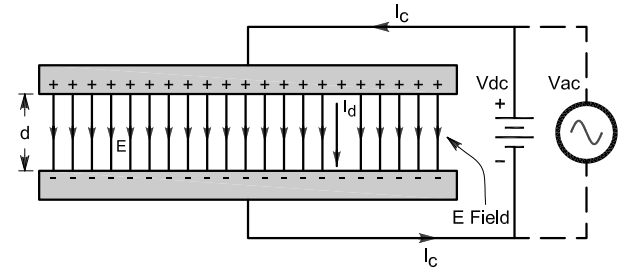

Fig 3—Example of an electric field, $E=V_{dc}/d$. When the dc source is replaced with an ac source there will be a displacement current (I_d) flowing between the capacitor plates.

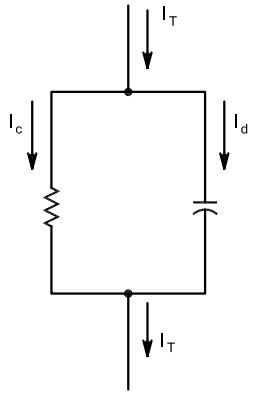

Fig 4—When the capacitor dielectric is less than perfect there will be a conduction current (I_c) in addition to the displacement current (I_d). Soil will typically have both resistive and capacitive components. Power loss in the soil is due to the current flowing through the resistive component.

A Closer Look at Verticals

A vertical antenna has two field components that induce currents in the ground around the antenna. **Fig 5** shows in a general way the electric-field component (E_z, in V/m) and magnetic-field component (H_ϕ, in A/m) in the region near a vertical. Because the soil near the antenna usually has relatively high resistance, both of these field components will induce currents (I_V and I_H) in the ground, resulting in losses. While the worms may enjoy the heated ground, power dissipated in the ground is subtracted from the radiated power, weakening your signal.

As shown in Fig 5, the tangential component of the H-field (H_ϕ) induces horizontal currents (I_H) flowing radially. The normal component (perpendicular to the ground surface) of the E-field (E_z) induces vertically flowing currents (I_v). Actually, things are more complex than this but we don't need to thrash through that to understand conceptually what's going on.

When modeling an antenna we account for the radiated power (P_r) by assuming there is a resistor we call the *radiation resistance* (R_r) through which the antenna base current (I_o) flows. The radiated power is then $P_r = I_o^2 R_r$. Similarly, we can account for the power dissipated in the ground (P_g) by adding a loss resistance (R_g) in series with R_r. The ground loss is then $P_g = I_o^2 R_g$. Additional losses due to conductors, loading coils, etc can also be simulated

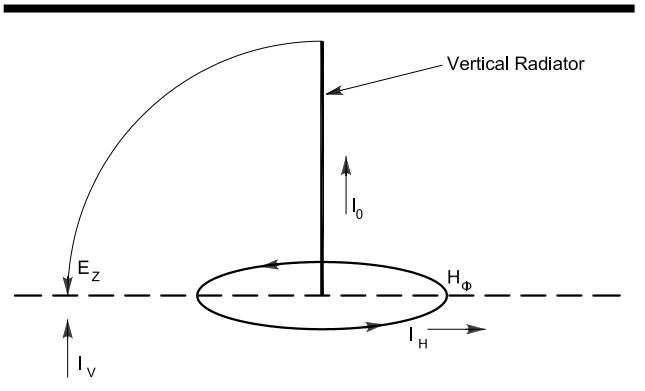

Fig 5—A general view of the fields and ground currents near the base of a vertical antenna. Note that the H-field distribution is equivalent to that shown in Fig 3.

by adding more series loss resistances. Putting aside for the moment these additional losses, the efficiency (η) of a vertical can be expressed as:

$$\eta = \frac{P_r}{P_r + P_g} \qquad \text{(Eq 1)}$$

This can be restated in terms of resistances as:

$$\eta = \frac{R_r}{R_r + R_g} = \frac{1}{1 + \frac{R_g}{R_r}} \qquad \text{(Eq 2)}$$

In essence, efficiency is the ratio of the radiated power to the total input power ($P_T = P_r + P_g$). Another way of saying this is that efficiency depends on the ratio of ground loss resistance (R_g) to radiation resistance (R_r), as Eq 2 shows. The smaller we make R_g the more power will be radiated for a given input power. Reducing R_g is the purpose of the ground system.

A sketch of current flow in the antenna and the surrounding ground (due to H-field), near the base of a vertical, is shown in **Fig 6**. I_z represents the total *zone current* flowing radially through a cylindrical zone at a given radius (r) due to the H field, while I_o is the current at the feed point at the base of the antenna. Technically speaking, the cylinder is infinitely deep, with I_z being the total current integrated over the surface of the cylinder at a given radius.

Fig 7 is a graph of the amplitude of I_z for several antenna heights in wavelengths (h) as we move away from the base of the antenna. Fig 7 shows the zone current that would flow in the ground returning to the base of the antenna, assuming a single ground rod is placed at the feed point for the vertical radiator. The heights indicated are the effective electrical heights. For example, if you use some top loading on the vertical, the effective electrical height will be greater than the physical height.

It is important to recognize that simply adding a top hat to a vertical of a given physical height may reduce ground losses. We can see this from the effect of h on ground current amplitude in Fig 7. Increasing h reduces the ground current. Even something as simple as moving a loading coil from the base up to the center of the antenna may reduce ground losses because it reduces ground current amplitude. But we do have to be careful that the loss introduced by the loading coil does not overcome the reduction in ground loss! Both loading-coil and top-hat schemes also increase the radiation resistance R_r, which further improves efficiency.

The currents in Fig 7 have been adjusted for constant radiated power at the base of the antenna by varying I_o to compensate for the change in R_r as we vary h. To maintain constant radiated power as R_r is falling, you must increase I_o. The base feed-point impedance is a strong function of h. For example, for h = 0.25 λ, R_r will be in the neighborhood of 36 Ω. However, for h = 0.1 λ, R_r will be less than 4 Ω. More information on short antennas can be found in Chapter 16, Mobile and Maritime Antennas.

Fig 7 clearly shows the high currents that flow in the ground near the base of a short antenna due to the antenna's H field. Compared to a 0.25-λ vertical, the 0.1-λ vertical has about three times the base current. As you shorten the antenna further, the zone current increases even more quickly. The ground loss is proportional to the square of the ground current ($P_g = I_g^2 R_g$), so the power loss in the immediate

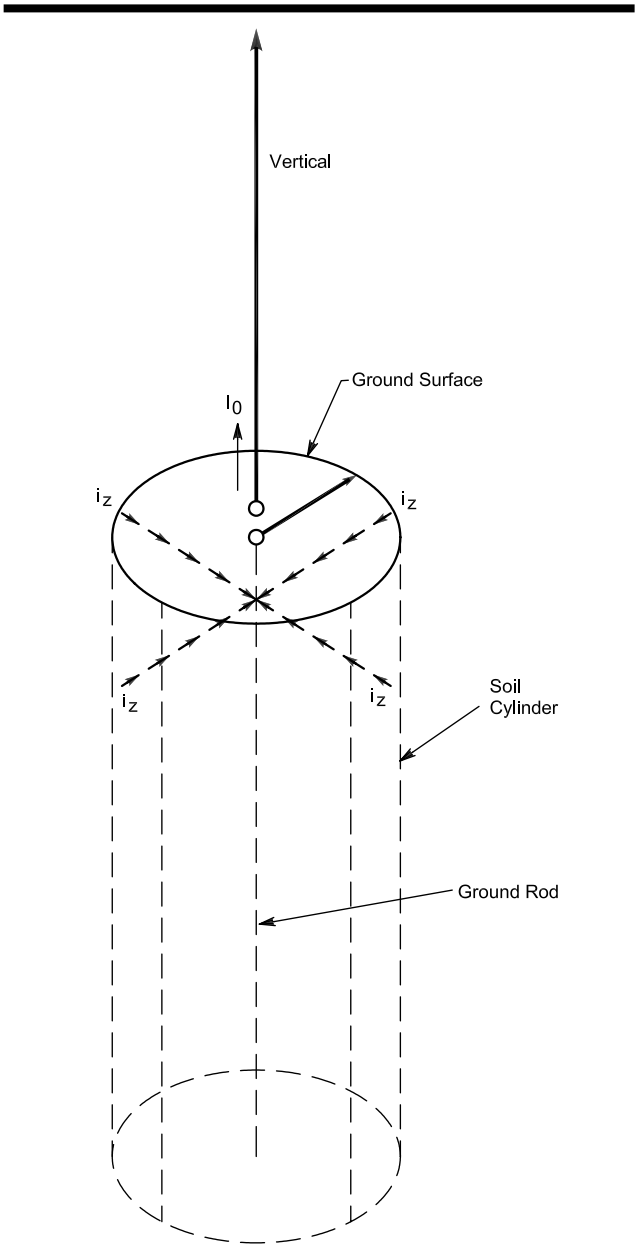

Fig 6—Representation of the zone current near the base of a vertical antenna. Individual i_z components of current flow into a cylinder of soil, with a radius r centered on the base of the vertical. The total current, I_z, thus represents the net current induced in the soil by the H-field for a given radius. (I_z was labeled I_H in Fig 5.)

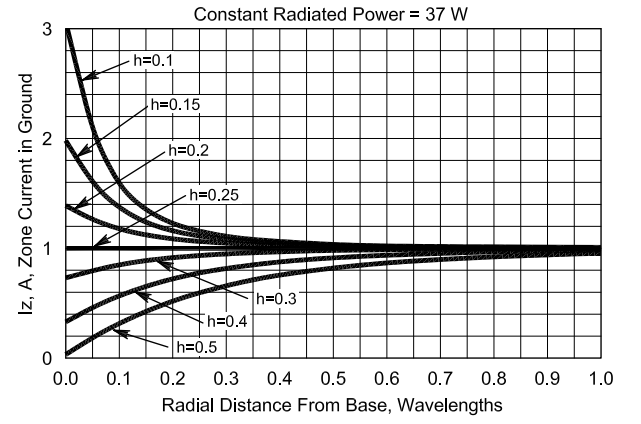

Fig 7—Plot of zone current (I_z) in amperes near the base of a vertical as a function of height (h) and radius (r) in wavelengths. The current in the base of the 0.25-λ antenna is assumed to be 1 A and the current for other values of h is adjusted to maintain the same radiated power ($P_r = I_o^2 R_r$ = 37 W) as the radiation resistance (R_r) changes with h.

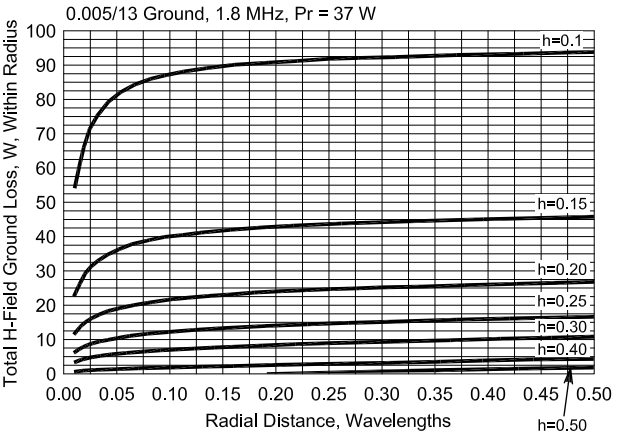

Fig 8—Total H-field induced ground loss within a circle of radius r around the base of a vertical for different values of h and constant P_r = 37 W. Note how the total loss increases rapidly near the base of the antenna indicating high loss. Beyond r = 0.15 λ, however, the additional loss is much lower and the curves flatten out. Note also how much higher the loss is for shorter antennas.

region of the base is much higher for a short antenna operating with the same input power as for a quarter-wave vertical.

We can calculate the losses induced in the soil by either the E- or H-field intensity. **Fig 8** shows an example of the H-field losses for several different antenna heights, given a constant radiated power of 37 W. Note that the total loss within 0.5 λ of the base for h = 0.25 λ is about 16 W (right side of the graph). This gives η = 37/(37 + 16) = 70%. However, for h = 0.1 λ, the total loss is about 94 W. Taking into consideration only the H-field losses, η = 37/(37 + 94) = 28%. Note that in both cases the majority of the loss is near (< 0.1 λ) the antenna, with the rate of increase of total loss decreasing rapidly as we move farther away from the base, where the lines are almost flat.

Fig 9 is a graph of the E-field intensity around a vertical with 1500 W radiated power, for three values of h. The E-field intensity doesn't depend on the exact type of ground system. (You can see this when you consider that the voltage across a capacitor doesn't depend on the size of the capacitor's plates.) Notice that close to the base, the E-field intensity for the 0.1-λ vertical is almost 100 times that for the 0.25-λ vertical. Because loss is proportional to the square of the voltage, the E-field losses close to the base will be ten thousand times larger in the 0.1-λ vertical! At a 1500-W power level the field intensity near the base of a short vertical is high enough to pose some risk of igniting grass and bushes that grow above any radial system close to the vertical's base. The grass should be kept mowed within 0.1 λ of the base.

Fig 10 shows a computation for the E-field losses, again for a constant radiated power of 37 W and several values of h. For the 0.25-λ vertical, the electric field intensity is quite low and so are the losses associated with it, at only 1.5 W.

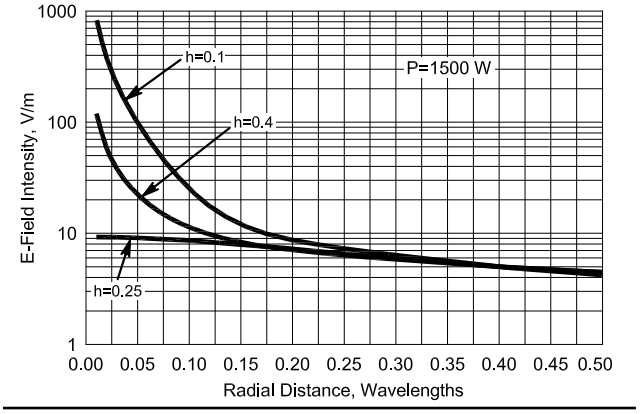

Fig 9—Electric field intensity near the base of a vertical for different values of h. P_r is held constant at 1500 W.

With any reasonable ground system, the E-field losses for a 0.25-λ vertical will be insignificant.

For shorter or longer verticals, however, the picture is different. This is why we see the very high losses (> 100 W) in Fig 10 for h = 0.1 λ. This loss, when added to the H-field loss, reduces the efficiency of the 0.1-λ vertical to 16% or less without a good ground system. In short antennas the E-field losses cannot be ignored, since they get worse exponentially as the antenna is shortened further.

The presence of a top-loading hat will also increase the E-field intensity in the area below the hat. However, most practical amateur hats will be quite small and the associated E-field loss small. The benefit, however, of reducing I_o because of the addition of the hat—which reduces the field

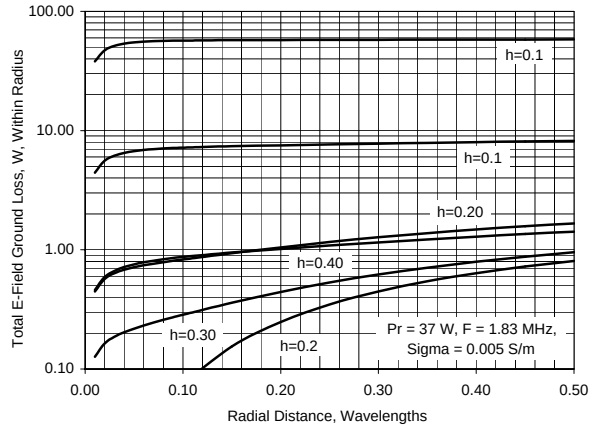

Fig 10—Total E-field induced ground loss within a circle of radius r around the base of a vertical for different values of h and constant P_r = 37 W. Note how the total loss increases rapidly near the base of the antenna, indicating high loss. Beyond r = 0.05 λ, however, the additional loss is much lower and the curves flatten out. Note again how much higher the loss is for shorter antennas. For h = 0.1 λ the E-field loss is greater than the H-field loss.

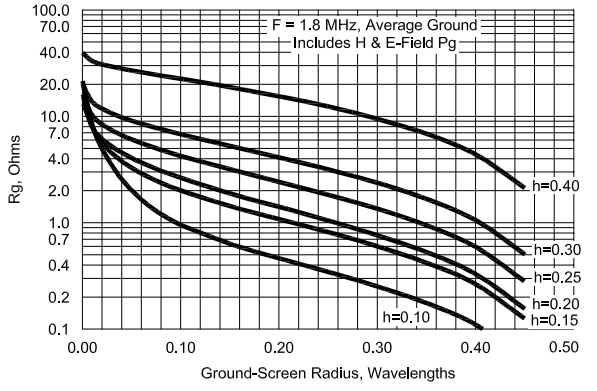

Fig 11—Effective ground resistance (R_g) at the base of the vertical as a function of the radius of a ground screen for several different antenna heights. Note how R_g falls as power dissipation in the soil is eliminated by the highly conducting ground screen.

from the vertical part of the antenna—more than compensates for the small additional E-field loss due to the hat.

Verticals taller than 0.25 λ also display increased E-field intensity, but not nearly so severe as short verticals. In verticals both shorter and longer than a 0.25 λ, the critical loss region is within a radius of about 0.05 λ. We can see this in Fig 10, where the power-loss curves for the shorter antennas flatten out by the time we reach a radius of 0.05 λ.

It's not widely known, but while radial wire systems reduce the H-field losses very effectively, Larsen (see Bibliography) has shown that the E-field losses with the same radial system do not fall in the same fashion as H-field losses. For h > 0.15 λ this doesn't matter much because the E-field loss is so low anyway. However, for short antennas it is very helpful to install either a ground screen or a dense radial system within 0.05 λ of the base.

We can take the data in Figs 8 and 10 and calculate the effective value of the ground resistance R_g. **Fig 11** shows the results of such a computation. Fig 11 assumes a perfect ground screen that varies in radius from 0.001 λ to 0.5 λ. As we would expect, when the ground screen is very small the ground losses are high, meaning R_g is high and the efficiency is low. As we increase the radius of the ground screen, forcing current out of the lossy soil and into the very low-loss screen, R_g drops rapidly and the efficiency increases.

Fig 11 demonstrates why it is desirable to have a good ground system out to at least 0.125 λ, and better yet, even farther. The shorter the antenna, the more important the ground system becomes, especially close to the base. In this example the ground system consists of a highly conductive, bonded ground screen, not always practical for amateur installations. A more typical ground system would consist of a number of individual radial wires. This kind of ground will be inferior to a screen but represents a practical compromise. We'll examine this in more detail shortly.

Note that as we reduce h in Fig 11, R_g actually goes down—even though the ground losses are higher. When h is made smaller the radiation resistance declines rapidly (see Chapter 16, Mobile and Maritime Antennas), so that for a given radiated power I_o must increase. If we measure R_g as we reduce h over a given ground system, we would see that the value for R_g goes down as shown in Fig 11. But because I_o^2 is rising more rapidly than R_g is falling, the power lost in the ground increases and efficiency decreases. The point here is that the value of R_g depends on the ground system, soil characteristics *and* the antenna configuration. You cannot assign an arbitrary value to R_g independent of the antenna system.

Wire Radial Systems

Fig 11 shows R_g for a dense, perfectly conducting ground screen, but what we really need to know is the effect of length and number of individual radials on R_g in a wire radial system. We can calculate the current division between a radial system and the soil and use this to determine R_g. A typical graph of the proportion of the zone current flowing in the radial system, as a function of radius and various numbers of radials (N), is shown in **Fig 12**.

The radial currents decrease as we move away from the base, and the lower the number of radials, the more rapidly the radial current decreases. This means that close to the base of the antenna most of the current is in the radial system, but as we move away from the base the current increasingly flows in the lossy ground. When only a few radials are used, the outer ends of the radials contribute little to reducing ground loss.

Why is this? The problem is that I_z does not go immediately to the nearest radial but may flow for some distance in the soil. This is illustrated in a general way in **Fig 13**. As

we move away from the base of the antenna, adjacent radials are further apart from each other and the current must flow further in the soil before it reaches one of the radials. When we use more radials, the distance between radials is less and more of the total current will be in the radials and less in the soil. This reduces ground loss.

When we know the current distribution in the ground we can calculate the power loss and R_g. A typical example for h = 0.25 λ is given in **Fig 14**. We can learn a lot about radial system design from Fig 14 and similar graphs. If we use only a few radials, the radial current drops off very rapidly. Most of the current is flowing in the soil.

Such a ground system is by nature inefficient—that is, R_g is large. We can also see that if we have only 16 radials, R_g falls an ohm or two as we lengthen the radials, but is essentially flat by 0.1 λ. There is no point in making them longer because there is little current in the outer portions and R_g is essentially constant beyond 0.1 λ. As we increase the number of radials, we gather more current further out, making longer radials more useful. The result is cumulative—more radials allow longer radials to be effective and both together reduce ground loss. We can see this in Fig 14, where the initial value of R_g drops as N increases and flattens out at longer radial lengths. For 128 radials, for example, lengths of 0.25 λ or more are useful.

The example in Fig 14 uses #12 wire for the radials. Compared to soil, the resistance of the radial wires is very small, especially if many radials are used, and does not greatly affect overall losses no matter how small the wire. The effect of changing wire size is to slowly change the current division between ground and the radial system. Larger wire results in only a small decrease in R_g. In principle, very small wire could be used for radials but from a mechanical point of view, #18 or #20 wire is about as small as is practical. Any smaller wire breaks too easily to be buried, and also breaks easily when left on the ground surface and is walked on or driven over.

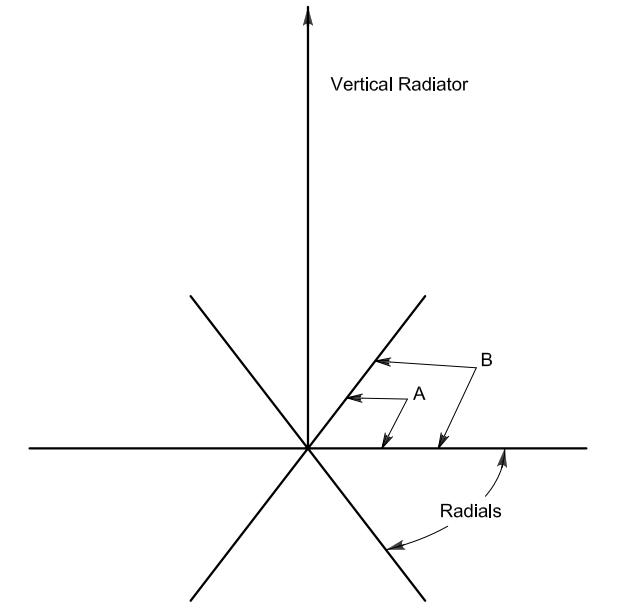

Fig 13—An example of current entering the ground between the radials and flowing for some distance before being picked up by a radial.

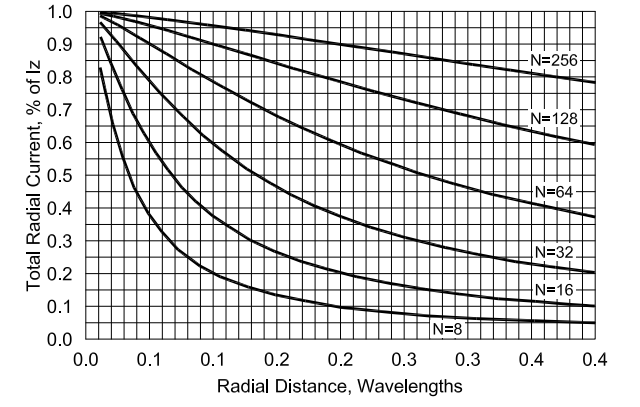

Fig 12—An example of the portion of the zone current flowing in the radial system as you move away from the base of a 0.25 λ vertical for different numbers of radials (N). Note that when more radials are used, more of the zone current flows in the radials and not in the ground, reducing ground loss. The proportion of current in the radial system falls rapidly when only a few radials are used. This leads to high ground loss because most of the zone current is flowing in the ground rather than in the radials.

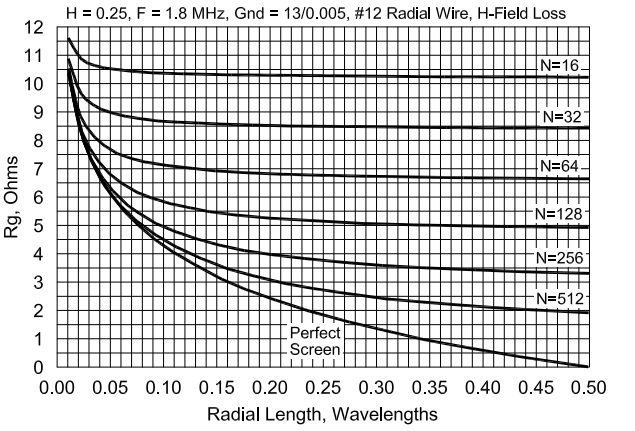

Fig 14—An example of the variation of R_g with radial length and number of radials (N) for h = 0.25 λ. When only a few radials are used there is little point in making them longer than 0.1 λ. Increasing N reduces R_g at a given radius and also makes longer radials useful, further reducing R_g. R_g for other values of h behave similarly.

On the other hand, wire larger than #12 is expensive. Thousands of feet of #8 wire may be affordable for broadcast stations but not for most hams. Increasing the wire size from #20 to #10 would result in only a small reduction in R_g. Of course, if you happen to have a few thousand feet of old RG-8 cable lying around (the diameter is comparable to #0000 wire) then that might indeed help to reduce R_g, as W9QQ has shown (see Bibliography). You are still better off, however, using many radials with small wire than a few radials with large wire. Radial wire size is usually a mechanical and financial issue, not an electrical one.

If the example in Fig 14 were changed for different ground characteristics, then the curves would have a similar shape but would be shifted either up or down. For example, poorer ground will result in higher R_g but the usable length for the radials for a given N would increase somewhat. For better-quality ground, with higher conductivity, R_g will be lower but the usable length of the radials for a given N will be shorter.

For short antennas, the initial drop in R_g will be more rapid and the curves flatten out sooner. This implies that somewhat shorter radials are useful with short antennas. However, given the high losses, it is still a very good idea to use lots of radials with short antennas. As in the above example, increasing N also increases the usable length.

As you go up in frequency from 160 meters, R_g generally rises slowly and then stabilizes around 7 MHz, depending on the ground characteristics. This effect is related to the change in skin depth with frequency, which is discussed in a later section of this chapter. There is also a small shift in current division between the radials and ground as the frequency increases.

A Word Of Caution

In the preceding discussion we presented a number of graphs and the CD-ROM accompanying this book contains some spreadsheets containing the equations from which these graphs were derived. From these graphs we extracted a number of observations on how to design radial systems. Basic to each graph is the assumption that we know the ground characteristics: conductivity and permitivity. In the real world, we amateurs very rarely have more than a rough idea of the ground characteristics under our antennas. Even when careful measurements are made, the characteristics will vary through the year with rainfall or the lack thereof.

Soils are always stratified vertically and can vary by factors or two or more horizontally over distances comparable to radial length, so that even good ground measurements are at best an average. In addition, there will frequently be constraints on the size and shape of the ground system. As a result, we use the calculated information and the previous graphs for general guidance and preliminary design, but when actually installing a ground system we try to measure—or at least estimate—R_g as we go along.

When R_g stops falling, or our patience and/or money run out, we stop adding ground radials. We can measure the feed-point resistance with an impedance bridge to estimate of R_g. The impedance seen at the feed point of the antenna is the sum of the loss and the radiation resistance. To determine R_g you have to estimate R_r (from the antenna height) and other losses due to loading or conductors, and then subtract that from the total measured input resistance. The remainder is R_g, and R_g should fall as we add radials. When R_g stops falling we probably have as many radials of a given length as will be useful. Further reduction in R_g would require more, longer radials.

Practical Suggestions For Vertical Ground Systems

At least 16 radials should be used if at all possible. Experimental measurements and calculations show that with this number, the loss resistance decreases the antenna efficiency by 30% to 50% for a 0.25 λ vertical, depending on soil characteristics. In general, a large number of radials (even though some or all of them must be short) is preferable to a few long radials for a vertical antenna mounted on the ground. The conductor size is relatively unimportant as mentioned before: #12 to #22 copper wire is suitable.

Table 1 summarizes these conclusions. John Stanley, K4ERO, first presented this material in December 1976 *QST*. Another source of information on ground-system design is *Radio Broadcast Ground Systems* (see the Bibliography at the end of this chapter). Most of the data presented in Table 1 is taken from that source, or derived from the interpolation of data contained therein.

Table 1 is based on the number of radials. For each configuration, there is a corresponding optimum radial length. Each configuration also includes the amount of wire used, expressed in wavelengths. Using radials considerably longer than suggested for a given N or using a lot more radials than suggested for a given length, while not adverse to performance, does not yield significant improvement either. That would represent a non-optimum use of wire and construction time. Each suggested configuration represents an optimum relationship between length and number for the given amount of total wire used. Table 1 leads to these conclusions:

- If you install only 16 radials (in configuration A), they need not be very long—0.1 λ is sufficient. The total length of wire will be 1.6 λ, which is about 875 feet at 1.8 MHz.
- If you have the wire, the space and the patience to lay down 120 radials (optimal configuration F), they should be 0.4 λ long. This radial system will gain about 3 dB over the 16-radial case and you'll use 48 λ of wire, or about 26,000 feet at 1.8 MHz.
- If you install 36 radials that are 0.15 λ long, you will lose 1.5 dB compared to optimal configuration F. You will use 5.4 λ of wire, or almost 3,000 feet at 1.8 MHz.

The loss figures in Table 1 assume h = 0.25 λ. A very rough approximation of loss when using shorter antennas can be obtained by doubling the loss in dB each

Table 1
Optimum Ground-System Configurations

	Configuration Designation					
	A	*B*	*C*	*D*	*E*	*F*
Number of radials	16	24	36	60	90	120
Length of each radial in wavelengths	0.1	0.125	0.15	0.2	0.25	0.4
Spacing of radials in degrees	22.5	15	10	6	4	3
Total length of radial wire installed, in wavelengths	1.6	3	5.4	12	22.5	48
Power loss in dB at low angles with a quarter-wave radiating element	3	2	1.5	1	0.5	0*
Feed-point impedance in ohms with a quarter-wave radiating element	52	46	43	40	37	35

Note: Configuration designations are indicated only for text reference.
*Reference: The loss of this configuration is negligible compared to a perfectly conducting ground.

time the antenna height is halved. For taller antennas the losses decrease, approaching 2 dB for configuration A of Table 1 for a half-wave radiator. Even longer antennas yield correspondingly better performance.

Table 1 is based on average ground conductivity. Variation of the loss values shown can be considerable, especially for configurations using fewer radials. Those building antennas over dry, sandy or rocky ground should expect more loss. On the other hand, higher than average soil conductivity and wet soils would make the compromise configurations (those with the fewest radials) even more attractive.

When antennas are combined into arrays, either parasitic or all-driven types, mutual impedances lower the radiation resistance of the elements. This drastically increases the effects of ground loss because I_o will be higher for the same power level. For instance, an antenna with a 50-Ω feed-point impedance, of which 10 Ω is ground-loss resistance, will have an efficiency of approximately 83%. An array of two similar antennas in a driven array with similar ground losses may have an efficiency of 70% or less.

Special precautions must be taken in such cases to achieve satisfactory operation. Generally speaking, a wide-spaced broadside array presents little problem because R_r is high, but a close-spaced end-fire array should be avoided because R_r is much lower, unless low-loss radial system configurations are used or other precautions taken. Chapter 8, Multielement Arrays, covers the subject of vertical arrays in great detail.

In cases where directivity is desirable or real-estate limitations dictate, longer, more closely spaced radials can be installed in one direction, and shorter, more widely spaced radials in another. Multiband ground systems can be designed using different optimum configurations for different bands. Usually it is most convenient to start at the lowest frequency with fewer radials and add more short radials for better performance on the higher bands.

There is nothing sacred about the exact details of the configurations in Table 1, and small changes in the number of radials and lengths will not cause serious problems. Thus, a configuration with 32 or 40 radials of 0.14 λ or 0.16 λ will work as well as configuration C shown in the table.

If less than 90 radials are contemplated, there is no need to make them a quarter wavelength long. This differs rather dramatically from the case of a ground-plane antenna, where resonant radials are installed above ground. For a ground-mounted antenna, quarter-wave long radials may not be optimum. Because the radials of a ground-mounted vertical are actually on, if not slightly below the surface, they are coupled by capacitance or conduction to the ground, and thus resonance effects are not important. The basic function of radials is to provide a low-loss return path for ground currents.

Radio Broadcast Ground Systems states, "Experiments show that the ground system consisting of only 15 radial wires need not be more than 0.1 wavelength long, while the system consisting of 113 radials is still effective out to 0.5 wavelength." Many graphs in that publication confirm this statement. This is not to say that these two systems will perform equally well; they most certainly will not. However, if 0.1 λ is as long as the radials can be, there is little point in using more than 15 of them unless the vertical radiator's height is also small.

The antenna designer should:

1. Study the cost of various radial configurations versus the gain of each.
2. Compare alternative means of improving transmitted signal and their cost (more power, etc).
3. Consider increasing the physical antenna height (the electrical length) of the vertical radiator, instead of improving the ground system.
4. Use multi-element arrays for directivity and gain, observing the necessary precautions related to mutual impedances discussed in Chapter 8, Multielement Arrays.

The Effect of Ground in the Far Field

The properties of the ground in the far field of an antenna are very important, especially for a vertically polarized antenna, as discussed above. Even if the ground-radial system for a vertical has been optimized to reduce ground-return losses in the reactive near field to an insignificant level, the electrical properties of the ground may still diminish far-field performance to lower levels than "perfect-ground" analyses might lead you to expect. The key is that *ground reflections* from horizontally and vertically polarized waves behave very differently.

Reflections in General

First, let us consider the case of flat ground. Over flat ground, either horizontally or vertically polarized downgoing waves launched from an antenna into the far field strike the surface and are reflected by a process very similar to that by which light waves are reflected from a mirror. As is the case with light waves, the angle of reflection is the same as the angle of incidence, so a wave striking the surface at an angle of, say, 15° is reflected upward from the surface at 15°.

The reflected waves combine with direct waves (those radiated at angles above the horizon) in various ways. Some of the factors that influence this combining process are the height of the antenna, its length, the electrical characteristics of the ground, and as mentioned above, the polarization of the wave. At some elevation angles above the horizon the direct and reflected waves are exactly in phase—that is, the maximum field strengths of both waves are reached at the same time at the same point in space, and the directions of the fields are the same. In such a case, the resultant field strength for that angle is simply the sum of the direct and reflected fields. (This represents a theoretical increase in field strength of 6 dB over the free-space pattern at these angles.)

At other elevation angles the two waves are completely out of phase—that is, the field intensities are equal at the same instant and the directions are opposite. At such angles, the fields cancel each other. At still other angles, the resultant field will have intermediate values. Thus, the effect of the ground is to increase radiation intensity at some elevation angles and to decrease it at others. When you plot the results as an elevation pattern, you will see *lobes* and *nulls*, as described in Chapter 2, Antenna Fundamentals.

The concept of an *image antenna* is often useful to show the effect of reflection. As **Fig 15** shows, the reflected ray has the same path length (AD equals BD) that it would if it originated at a virtual second antenna with the same characteristics as the real antenna, but situated below the ground just as far as the actual antenna is above it.

Now, if we look at the antenna and its image over perfect ground from a remote point on the surface of the ground, we will see that the currents in a horizontally polarized antenna and its image are flowing in opposite directions, or in other words, are 180° out of phase. But the currents in a vertically polarized antenna and its image are flowing in the *same* direction—they are *in* phase. This 180° phase difference between the vertically and horizontally polarized reflections off ground is what makes the combinations with direct waves behave so very differently.

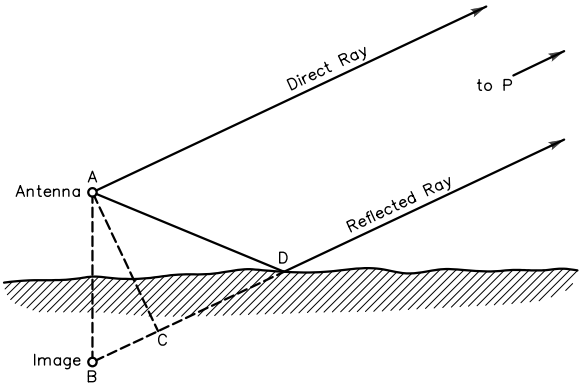

Fig 15—At any distant point, P, the field strength will be the vector sum of the direct ray and the reflected ray. The reflected ray travels farther than the direct ray by the distance BC, where the reflected ray is considered to originate at the *image* antenna.

FAR-FIELD GROUND REFLECTIONS AND THE VERTICAL ANTENNA

A vertical's azimuthal directivity is omnidirectional. A λ/2 vertical over ideal, perfectly conducting earth has the elevation-plane radiation pattern shown by the solid line in **Fig 16**. Over real earth, however, the pattern looks more like the shaded one in the same diagram. In this case, the low-angle radiation that might be hoped for because of perfect-ground performance is not realized in the real world.

Now look at **Fig 17A**, which compares the computed elevation-angle response for two half-wave dipoles at 14 MHz. One is oriented horizontally over ground at a height of λ/2 and the other is oriented vertically, with its center just over λ/2 high (so that the bottom end of the wire doesn't actually touch the ground). The ground is "average" in dielectric constant (13) and conductivity (0.005 S/m). At a 15° elevation angle, the horizontally polarized dipole has almost 7 dB more gain than its vertical brother. Contrast Fig 17A to the comparison in Fig 17B, where the peak gain of a vertically polarized half-wave dipole over seawater, which is virtually perfect for RF reflections, is quite comparable with the horizontal dipole's response at 15°, and exceeds the horizontally polarized antenna dramatically below 15° elevation.

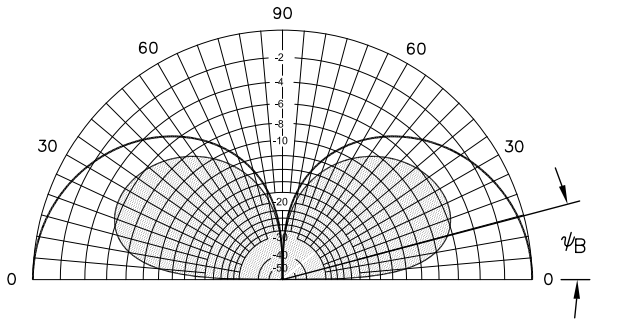

Fig 16—Vertical-plane radiation pattern for a ground-mounted quarter-wave vertical. The solid line is the pattern for perfect earth. The shaded pattern shows how the response is modified over average earth (k = 13, G = 0.005 S/m) at 14 MHz. ψ is the pseudo-Brewster angle (PBA), in this case 14.8°.

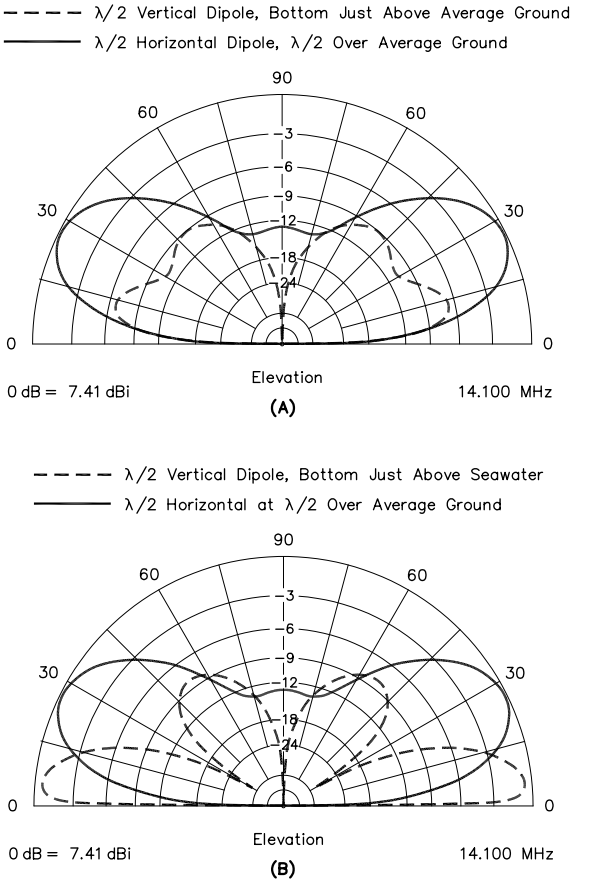

Fig 17—At A, comparison of horizontal and vertical λ/2 dipoles over average ground. Average ground has conductivity of 5 mS/m and dielectric constant of 13. Horizontal dipole is λ/2 high; vertical dipole's bottom wire is just above ground. Horizontal antenna is much less affected by far-field ground losses compared with its vertical counterpart. At B, comparison of 20-meter λ/2 vertical dipole whose bottom wire is just above seawater with λ/2-high horizontal dipole over average ground. Seawater is great for verticals!

To understand in a qualitative fashion why the desired low-angle radiation from a vertical is not delivered when the ground isn't "perfect," examine **Fig 18A**. Radiation from each antenna segment reaches a point P in space by two paths; one directly from the antenna, path AP, and the other by reflection from the earth, path AGP. (Note that P is so far away that the slight difference in angles is insignificant—for practical purposes the waves are parallel to each other at point P.)

If the earth were a perfectly conducting surface, there would be no phase shift of the vertically polarized wave upon reflection at point G. The two waves would add together with some phase difference because of the different path lengths. This difference in path lengths of the two waves is why the free-space radiation pattern differs from the pattern of the same antenna over ground.

Now consider a point P that is close to the horizon, as in Fig 18B. The path lengths AP and AGP are almost the same, so the magnitudes of the two waves add together, producing a maximum at zero angle of radiation. The arrows on the waves point both ways since the process works similarly for transmitting and receiving.

With real earth, however, the reflected wave from a vertically polarized antenna undergoes a change in both *amplitude* and *phase* in the reflection process. Indeed, at a low-enough elevation angle, the phase of the reflected wave will actually change by 180° and its magnitude will then subtract from that of the direct wave. At a zero takeoff angle, it will be almost equal in amplitude, but 180° out of phase with the direct wave.

Note that this is very similar to what happens with horizontally polarized reflected and direct waves at low elevation angles. Virtually complete cancellation will result in a deep null, inhibiting any radiation or reception at 0°. For real-world soils, the vertical loses the theoretical advantage it has at low elevation angles over a horizontal antenna, as Fig 17A so clearly shows.

The degree that a vertical works better than a horizontal antenna at low elevation angles is largely dependent on the characteristics of the ground around the vertical, as we'll next examine.

THE PSEUDO-BREWSTER ANGLE AND THE VERTICAL ANTENNA

Much of the material presented here regarding pseudo-Brewster angle was prepared by Charles J. Michaels, W7XC, and first appeared in July 1987 *QST*, with additional information in *The ARRL Antenna Compendium, Vol 3*. (See the Bibliography at the end of this chapter.)

Most fishermen have noticed that when the sun is low, its light is reflected from the water's surface as glare, obscuring the underwater view. When the sun is high, however, the sunlight penetrates the water and it is possible to see objects below the surface of the water. The angle at which this transition takes place is known as the *Brewster angle*,

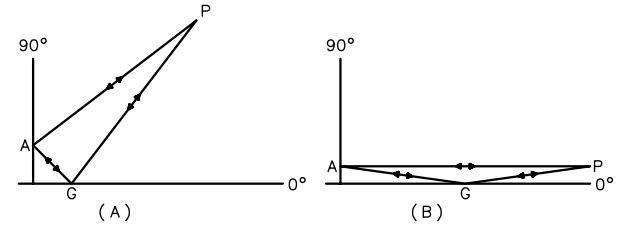

Fig 18—The direct wave and the reflected wave combine at point P to form the pattern (P is very far from the antenna). At A the two paths AP and AGP differ appreciably in length, while at B these two path lengths are nearly equal.

named for the Scottish physicist, Sir David Brewster (1781-1868).

A similar situation exists in the case of vertically polarized antennas; the RF energy behaves as the sunlight in the optical system, and the earth under the antenna acts as the water. The *pseudo-Brewster angle* (PBA) is the angle at which the reflected wave is 90° out of phase with respect to the direct wave. "Pseudo" is used here because the RF effect is similar to the optical effect from which the term gets its name. Below this angle, the reflected wave is between 90° and 180° out of phase with the direct wave, so some degree of cancellation takes place. The largest amount of cancellation occurs near 0°, and steadily less cancellation occurs as the PBA is approached from below.

The factors that determine the PBA for a particular location *are not related to the antenna itself, but to the ground around it*. The first of these factors is earth conductivity, G, which is a measure of the ability of the soil to conduct electricity. Conductivity is the inverse of resistance. The second factor is the dielectric constant, k, which is a unitless quantity that corresponds to the capacitive effect of the earth. For both of these quantities, the higher the number, the better is the ground (for vertical antenna purposes). The third factor determining the PBA for a given location is the frequency of operation. The PBA increases with increasing frequency, all other conditions being equal. **Table 2** gives typical values of conductivity and dielectric constant for different types of soil. The map of **Fig 19** shows the approximate conductivity values for different areas in the continental United States.

As the frequency is increased, the role of the dielectric constant in determining the PBA becomes more significant. **Table 3** shows how the PBA varies with changes in ground conductivity, dielectric constant and frequency. The table shows trends in PBA dependency on ground constants and frequency. The constants chosen are not necessarily typical of any geographical area; they are just examples.

At angles below the PBA, the reflected vertically polarized wave subtracts from the direct wave, causing the radiation intensity to fall off rapidly. Similarly, above the PBA, the reflected wave adds to the direct wave, and the radiated pattern approaches the perfect-earth pattern. Fig 16 shows the PBA, usually labeled ψ_B.

When plotting vertical-antenna radiation patterns over real earth, the reflected wave from an antenna segment is multiplied by a factor called the *vertical reflection coefficient*, and the product is then added vectorially to the direct wave to get the resultant. The reflection coefficient consists of an attenuation factor, A, and a phase angle, ϕ, and is usually expressed as $A\angle\phi$. (ϕ is always a negative angle, because the earth acts as a lossy capacitor in this situation.) The following equation can be used to calculate the reflection coefficient for vertically polarized waves, for earth of given conductivity and dielectric constant at any frequency and elevation angle (also called the wave angle in many texts).

Table 2
Conductivities and Dielectric Constants for Common Types of Earth

Surface Type	*Dielectric Constant*	*Conductivity (S/m)*	*Relative Quality*
Fresh water	80	0.001	
Salt water	81	5.0	
Pastoral, low hills, rich soil, typ Dallas, TX, to Lincoln, NE areas	20	0.0303	Very good
Pastoral, low hills, rich soil typ OH and IL	14	0.01	
Flat country, marshy, densely wooded, typ LA near Mississippi River	12	0.0075	
Pastoral, medium hills and forestation, typ MD, PA, NY, (exclusive of mountains and coastline)	13	0.006	
Pastoral, medium hills and forestation, heavy clay soil, typ central VA	13	0.005	Average
Rocky soil, steep hills, typ mountainous	12-14	0.002	Poor
Sandy, dry, flat, coastal	10	0.002	
Cities, industrial areas	5	0.001	Very Poor
Cities, heavy industrial areas, high buildings	3	0.001	Extremely poor

Table 3
Pseudo-Brewster Angle Variation with Frequency, Dielectric Constant, and Conductivity

Frequency (MHz)	*Dielectric Constant*	*Conductivity (S/m)*	*PBA (degrees)*
7	20	0.0303	6.4
	13	0.005	13.3
	13	0.002	15.0
	5	0.001	23.2
	3	0.001	27.8
14	20	0.0303	8.6
	13	0.005	14.8
	13	0.002	15.4
	5	0.001	23.8
	3	0.001	29.5
21	20	0.0303	10.0
	13	0.005	15.2
	13	0.002	15.4
	5	0.001	24.0
	3	0.001	29.8

$$A_{Vert} \angle \phi = \frac{k' \sin\psi - \sqrt{k' - \cos^2 \psi}}{k' \sin\psi + \sqrt{k' - \cos^2 \psi}} \quad \text{(Eq 3)}$$

where

$A_{Vert} \angle \phi$ = vertical reflection coefficient

ψ = elevation angle

$$k' = k - j\left|\frac{1.8 \times 10^4 \times G}{f}\right|$$

k = dielectric constant of earth (k for air = 1)

G = conductivity of earth in S/m

f = frequency in MHz

j = complex operator ($\sqrt{-1}$)

Solving this equation for several points indicates what effect the earth has on vertically polarized signals at a particular location for a given frequency range. **Fig 20** shows the reflection coefficient as a function of elevation angle at 21 MHz over average earth (G = 0.005 S/m, and k = 13).

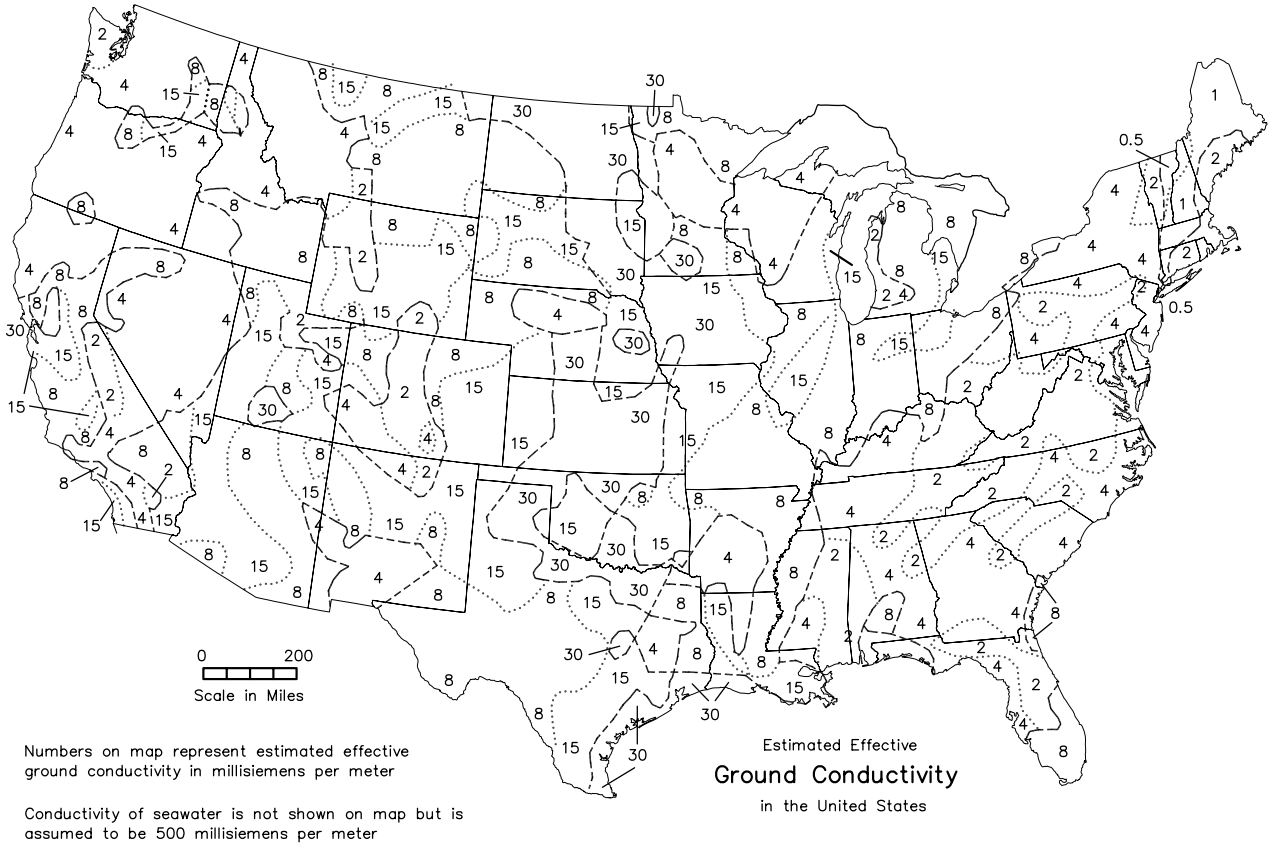

Fig 19—Typical average soil conductivities for the continental United States. Numeric values indicate conductivities in millisiemens per meter (mS/m), where 1.0 mS/m = 0.001 S/m.

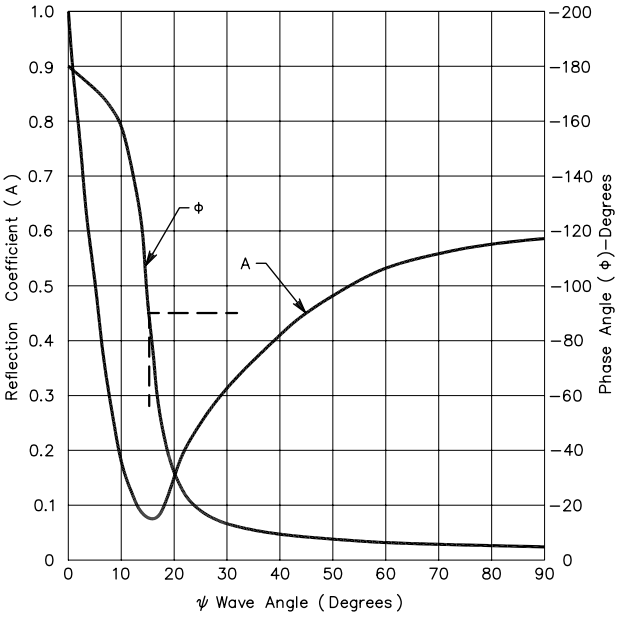

Fig 20—Reflection coefficient for vertically polarized waves. A and ϕ are magnitude and angle for wave angles ψ. This case is for average earth, (k = 13, G = 0.005 S/m), at 21 MHz.

Note that as the phase curve, ψ, passes through 90°, the attenuation curve (A) passes through a minimum at the same wave angle ψ. This is the PBA. At this angle, the reflected wave is not only at a phase angle of 90° with respect to the direct wave, but is so low in amplitude that it does not aid the direct wave by a significant amount. In the case illustrated in Fig 20 this elevation angle is about 15°.

Variations in PBA with Earth Quality

From Eq 3, it is quite a task to search for either the 90° phase point or the attenuation curve minimum for a wide variety of earth conditions. Instead, the PBA can be calculated directly from the following equation.

$$\psi_B = \arcsin\sqrt{\frac{k-1+\sqrt{(x^2+k^2)^2(k-1)^2+x^2[(x^2+k^2)^2-1]}}{(x^2+k^2)^2-1}} \qquad \text{(Eq 4)}$$

where k, G and f are as defined for Eq 3, and

$$x = \frac{1.8\times10^4\times G}{f}$$

Fig 21 shows curves calculated using Eq 4 for several different earth conditions, at frequencies between 1.8 and 30 MHz. As expected, poorer earths yield higher PBAs. Unfortunately, at the higher frequencies (where low-angle radiation is most important for DX work), the PBAs are highest. The PBA is the same for both transmitting and receiving.

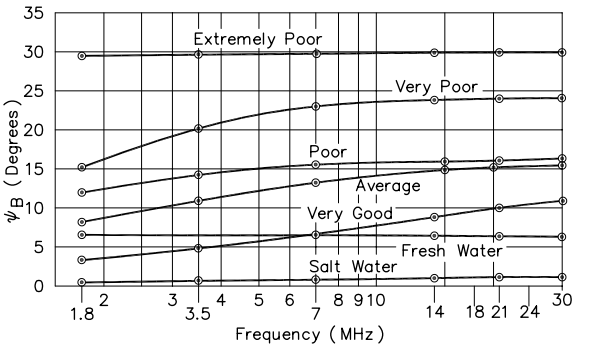

Fig 21—Pseudo-Brewster angle (ψ) for various qualities of earth over the 1.8 to 30-MHz frequency range. Note that the frequency scale is logarithmic. The constants used for each curve are given in Table 2.

Relating PBA to Location and Frequency

Table 2 lists the physical descriptions of various kinds of earth with their respective conductivities and dielectric constants, as mentioned earlier. Note that in general, the dielectric constants and conductivities are higher for better earths. This enables the labeling of the earth characteristics as extremely poor, very poor, poor, average, very good, and so on, without the complications that would result from treating the two parameters independently.

Fresh water and salt water are special cases; in spite of high resistivity, the fresh-water PBA is 6.4°, and is nearly independent of frequency below 30 MHz. Salt water, because of its extremely high conductivity, has a PBA that never exceeds 1° in this frequency range. The extremely low conductivity listed for cities (the last case) in Table 2 results more from the clutter of surrounding buildings and other obstructions than any actual earth characteristic. The PBA at any location can be found for a given frequency from the curves in Fig 21.

FLAT-GROUND REFLECTIONS AND HORIZONTALLY POLARIZED WAVES

The situation for horizontal antennas is different from that of verticals. **Fig 22** shows the reflection coefficient for horizontally polarized waves over average earth at 21 MHz. Note that in this case, the phase-angle departure from 0° never gets very large, and the attenuation factor that causes the most loss for high-angle signals approaches unity for low angles. Attenuation increases with progressively poorer earth types.

In calculating the broadside radiation pattern of a horizontal λ/2 dipole, the perfect-earth image current, equal to the true antenna current but 180° out of phase with it) is multiplied by the horizontal reflection coefficient given by Eq 5 below. The product is then added vectorially to the direct wave to get the resultant at that elevation angle. The

reflection coefficient for horizontally polarized waves can be calculated using the following equation.

$$A_{Horiz} \angle \phi = \frac{\sqrt{k' - \cos^2 \psi} - \sin \psi}{\sqrt{k' - \cos^2 \psi} + \sin \psi} \quad \text{(Eq 5)}$$

where

$A_{Horiz} \angle \phi$ = horizontal reflection coefficient

ψ = elevation angle

$$k' = k - j\left(\frac{1.8 \times 10^4 \times G}{f}\right)$$

k = dielectric constant of earth

G = conductivity of earth in S/m

f = frequency in MHz

j = complex operator ($\sqrt{-1}$)

For a horizontal antenna near the earth, the resultant pattern is a modification of the free-space pattern of the antenna. **Fig 23** shows how this modification takes place for a horizontal λ/2 antenna over a perfectly conducting flat surface. The patterns at the left show the relative radiation when one views the antenna from the side; those at the right show the radiation pattern looking at the end of the antenna. Changing the height above ground from λ/4 to λ/2 makes a significant difference in the high-angle radiation, moving the main lobe down lower.

Note that for an antenna height of λ/2 (Fig 23, bottom), the out-of-phase reflection from a perfectly conducting surface creates a null in the pattern at the zenith (90° elevation angle). Over real earth, however, a *filling in* of this null occurs because of ground losses that prevent perfect reflection of high-angle radiation.

At a 0° elevation angle, horizontally polarized antennas also demonstrate a null, because out-of-phase reflection cancels the direct wave. As the elevation angle departs from 0°, however, there is a slight filling-in effect so that over other-than-perfect earth, radiation at lower angles is enhanced compared to a vertical. A horizontal antenna will often outperform a vertical for low-angle DX work, particularly over lossy types of earth at the higher frequencies.

Reflection coefficients for vertically and horizontally polarized radiation differ considerably at most angles above ground, as can be seen by comparison of Figs 20 and 22. (Both sets of curves were plotted for the same ground constants and at the same frequency, so they may be compared directly.) This is because, as mentioned earlier, the image of a horizontally polarized antenna is out-of-phase with the antenna itself, and the image of a vertical antenna is in-phase with the actual radiator.

The result is that the phase shifts and reflection magnitudes vary greatly at different angles for horizontal and vertical polarization. The magnitude of the reflection coefficient for vertically polarized waves is greatest (near unity) at very low angles, and the phase angle is close to 180°. As mentioned earlier, this cancels nearly all radiation at very low angles. For the same range of angles, the magnitude of the reflection coefficient for horizontally polarized waves is also near unity, but the phase angle is near 0° for the specific conditions shown in Figs 20 and 22. This causes reinforcement of low-angle horizontally polarized waves. At some relatively high angle, the reflection coefficients for

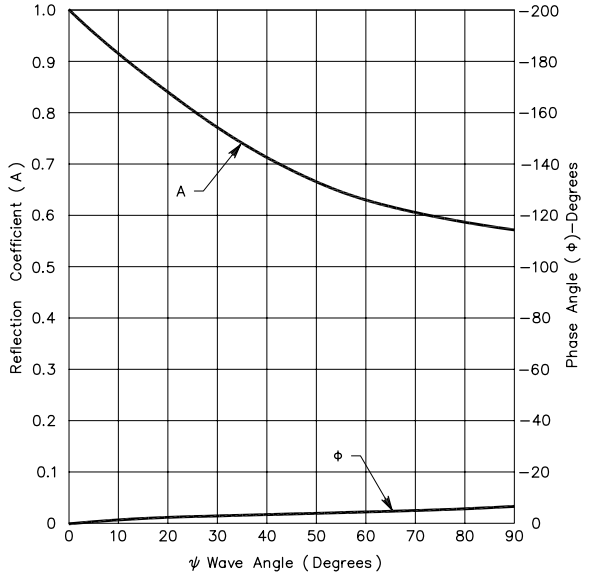

Fig 22—Reflection coefficient for horizontally polarized waves (magnitude A at angle ϕ), at 21 MHz over average earth (k = 13, G = 0.005 S/m).

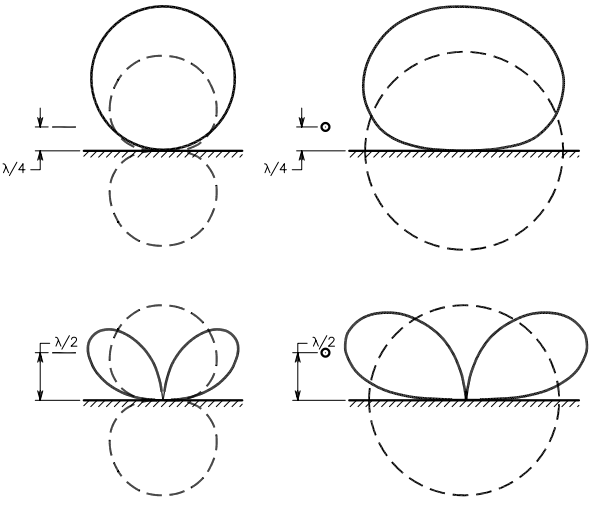

Fig 23—Effect of the ground on the radiation from a horizontal half-wave dipole antenna, for heights of one-fourth and one-half wavelength. Broken lines show what the pattern would be if there were no reflection from the ground (free space).

horizontally and vertically polarized waves are equal in magnitude and phase. At this angle (approximately 81° for the example case), the effect of ground reflection on vertically and horizontally polarized signals will be the same.

DEPTH OF RF CURRENT PENETRATION

When considering earth characteristics, questions about depth of RF current penetration often arise. For instance, if a given location consists of a 6-foot layer of soil overlying a highly resistive rock strata, which material dominates? The answer depends on the frequency, the soil and rock dielectric constants, and their respective conductivities. The following equation can be used to calculate the current density at any depth.

$$e^{-pd} = \frac{\text{Current Density at Depth d}}{\text{Current Density at Surface}} \qquad \text{(Eq 6)}$$

where

d = depth of penetration in cm

e = natural logarithm base (2.718)

$$p = \left(\frac{X \times B}{2} \times \left(\sqrt{1 + \frac{G^2 \times 10^{-4}}{B^2}} - 1 \right) \right)^{1/2}$$

$X = 0.008 \times \pi^2 \times f$

$B = 5.56 \times 10^{-7} \times k \times f$

k = dielectric constant of earth

f = frequency in MHz

G = conductivity of earth in S/m

After some manipulation of this equation, it can be used to calculate the depth at which the current density is some fraction of that at the surface. The depth at which the current density is 37% (1/*e*) of that at the surface (often referred to as *skin depth*) is the depth at which the current density would be zero if it were distributed uniformly instead of exponentially. (This 1/*e* factor appears in many physical situations. For instance, a capacitor charges to within 1/*e* of full charge within one RC time constant.) At this depth, since the power loss is proportional to the square of the current, approximately 91% of the total power loss has occurred, as has most of the phase shift, and current flow below this level is negligible.

Fig 24 shows the solutions to Eq 6 over the 1.8 to 30-MHz frequency range for various types of earth. For example, in very good earth, substantial RF currents flow down to about 3.3 feet at 14 MHz. This depth goes to 13 feet in average earth and as far as 40 feet in very poor earth. Thus, if the overlying soil is rich, moist loam, the underlying rock stratum is of little concern. However, if the soil is only average, the underlying rock may constitute a major consideration in determining the PBA and the depth to which the RF current will penetrate.

The depth in fresh water is about 156 feet and is nearly independent of frequency in the amateur bands below 30 MHz. In salt water, the depth is about seven inches at 1.8 MHz and decreases rather steadily to about two inches at 30 MHz. Dissolved minerals in moist earth increase its conductivity.

The depth-of-penetration curves in Fig 24 illustrate a noteworthy phenomenon. While skin effect confines RF current flow close to the surface of a conductor, the earth is so lossy that RF current penetrates to much greater depths than in most other media. The depth of RF current penetration is a function of frequency as well as earth type. Thus, the only cases in which most of the current flows near the surface are with very highly conductive media (such as salt water), and at frequencies above 30 MHz.

DIRECTIVE PATTERNS OVER REAL GROUND

As explained in Chapter 2, Antenna Fundamentals, because antenna radiation patterns are three-dimensional, it is helpful in understanding their operation to use a form of representation showing the elevation-plane directional characteristic for different heights. It is possible to show selected elevation-plane patterns oriented in various directions with respect to the antenna axis. In the case of the horizontal half-wave dipole, a plane running in a direction along the axis and another broadside to the antenna will give a good deal of information.

The effect of reflection from the ground can be expressed as a separate *pattern factor*, given in decibels. For any given elevation angle, adding this factor algebraically to the value for that angle from the free-space pattern for that antenna gives the resultant radiation value at that

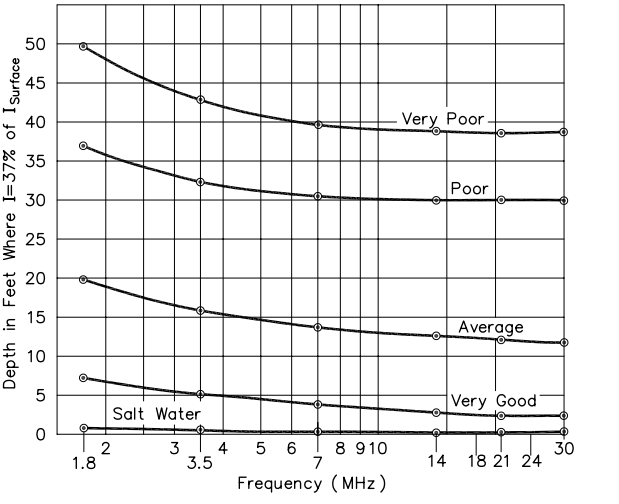

Fig 24—Depths at which the current density is 37% (1/*e*) of that at the surface for different qualities of earth over the 1.8- to 30-MHz frequency range. The depth for fresh water, not plotted, is 156 feet and almost independent of frequency below 30 MHz. See text and Table 2 for ground constants.

angle. The limiting conditions are those represented by the direct ray and the reflected ray being exactly in-phase and exactly out-of-phase, when both (assuming there are no ground losses) have equal amplitudes. Thus, the resultant field strength at a distant point may be either 6 dB greater than the free-space pattern (twice the field strength), or zero, in the limiting cases.

Horizontally Polarized Antennas

The way in which pattern factors vary with height for horizontal antennas over flat earth is shown graphically in the plots of **Fig 25**. The solid-line plots are based on perfectly conducting ground, while the shaded plots are based on typical real-earth conditions. These patterns apply to horizontal antennas of any length. While these graphs are, in fact, radiation patterns of horizontal single-wire antennas (dipoles) as viewed from the axis of the wire, it must be remembered that the plots merely represent pattern factors.

Fig 26 shows vertical-plane radiation patterns in the directions off the ends of a horizontal half-wave dipole for various antenna heights. These patterns are scaled so they may be compared directly to those for the appropriate heights in Fig 25. Note that the perfect-earth patterns in Figs 26A and 25B are the same as those in the upper part of Fig 23. Note also that the perfect-earth patterns of Figs 26B and 25D are the same as those in the lower section of Fig 23. The reduction in field strength off the ends of the wire at the lower angles, as compared with the broadside field strength, is quite apparent. It is also clear from Fig 26 that, at some heights, the high-angle radiation off the ends is nearly as great as the broadside radiation, making the antenna essentially an omnidirectional radiator.

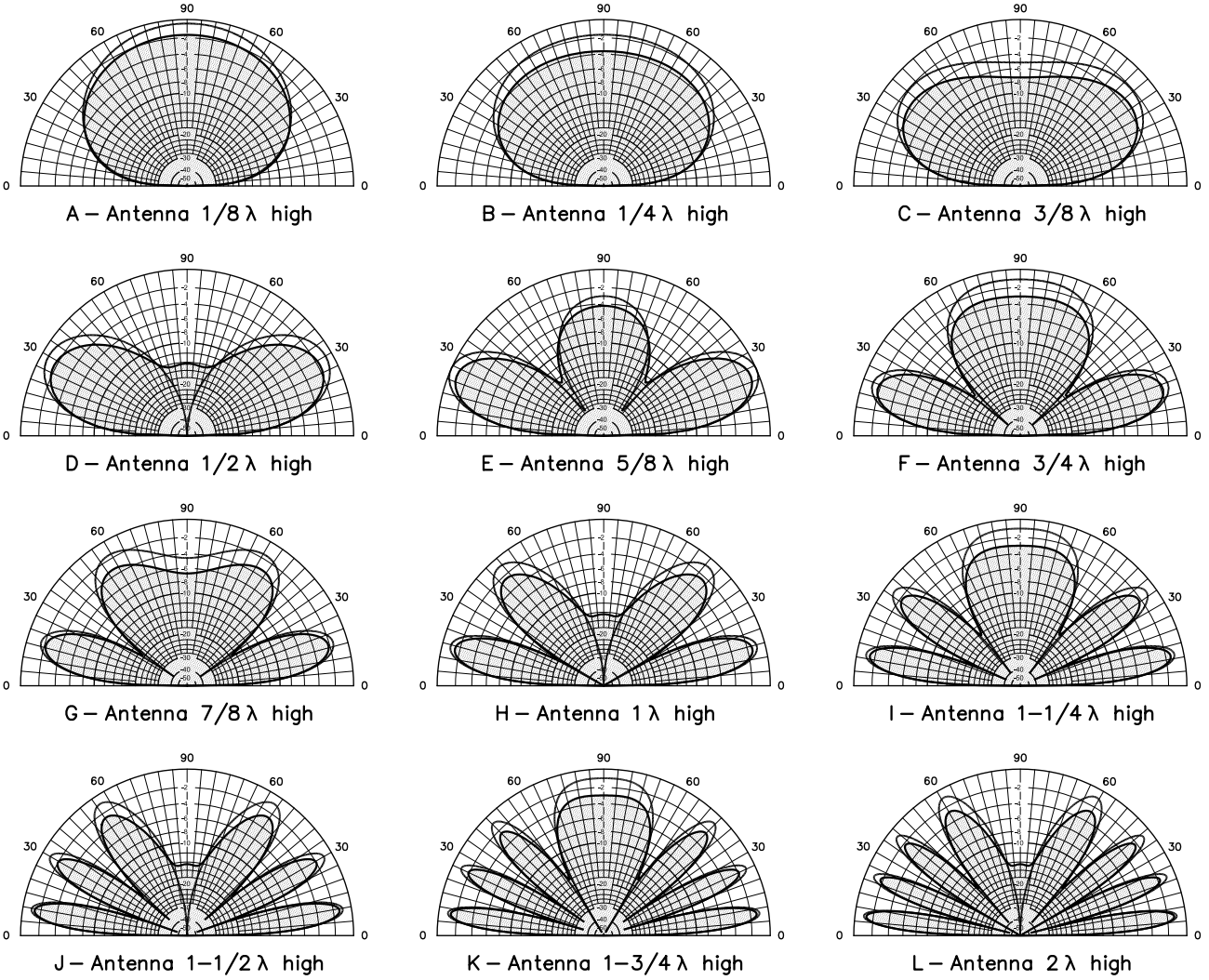

Fig 25—Reflection factors for horizontal dipole antennas at various heights above flat ground. The solid-line curves are the perfect-earth patterns (broadside to the antenna wire); the shaded curves represent the effects of average earth (k = 13, G = 0.005 S/m) at 14 MHz. Add 7 dB to values shown for absolute gain in dBd referenced to dipole in free space, or 9.15 dB for gain in dBi. For example, peak gain over perfect earth at $^5/_8$ λ height is 7 dBd (or 9.15 dBi) at 25° elevation.

In vertical planes making some intermediate angle between 0° and 90° with the wire axis, the pattern will have a shape intermediate between the broadside and end-on patterns. By visualizing a smooth transition from the end-on pattern to the broadside pattern as the horizontal angle is varied from 0° to 90°, a fairly good mental picture of the actual solid pattern may be formed. An example is shown in **Fig 27**. At A, the elevation-plane pattern of a half-wave dipole at a height of λ/2 is shown through a plane 45° away from the favored direction of the antenna. At B and C, the pattern of the same antenna is shown at heights of 3λ/4 and 1λ (through the same 45° off-axis plane). These patterns are scaled so they may be compared directly with the broadside and end-on patterns for the same antenna (at the appropriate heights) in Figs 25 and 26.

The curves presented in **Fig 28** are useful for determining heights of horizontal antennas that give either maximum or minimum reinforcement at any desired wave angle. For instance, if you want to place an antenna at a height so that it will have a null at 30°, the antenna should be placed where a broken line crosses the 30° line on the horizontal scale. There are two heights (up to 2 λ) that will yield this null angle: 1 λ and 2 λ.

As a second example, you may want to have the ground reflection give maximum reinforcement of the direct ray from a horizontal antenna at a 20° elevation angle. The antenna height should be 0.75 λ. The same height will give a null at 42° and a second lobe at 90°.

Fig 28 is also useful for visualizing the vertical pattern of a horizontal antenna. For example, if an antenna is erected at 1.25 λ, it will have major lobes (solid-line crossings) at 12° and 37°, as well as at 90° (the zenith). The nulls in this pattern (dashed-line crossings) will appear at 24° and 53°.

The Y-axis in Fig 28 plots the wave angle versus the height in wavelength above flat ground on the X-axis. Fig 28 doesn't show the elevation angles required for actual

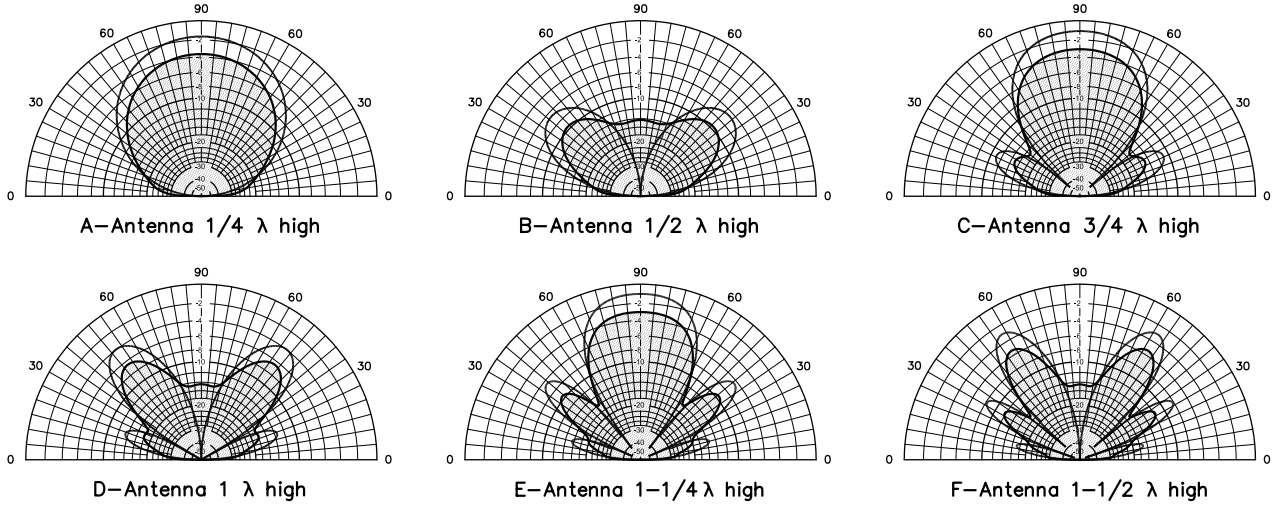

Fig 26—Vertical-plane radiation patterns of horizontal half-wave dipole antennas off the ends of the antenna wire. The solid-line curves are the flat, perfect-earth patterns, and the shaded curves represent the effects of average flat earth (k = 13, G = 0.005 S/m) at 14 MHz. The 0-dB reference in each plot corresponds to the peak of the main lobe in the favored direction of the antenna (the maximum gain). Add 7 dB to values shown for absolute gain in dBd referenced to dipole in free space, or 9.15 dB for gain in dBi.

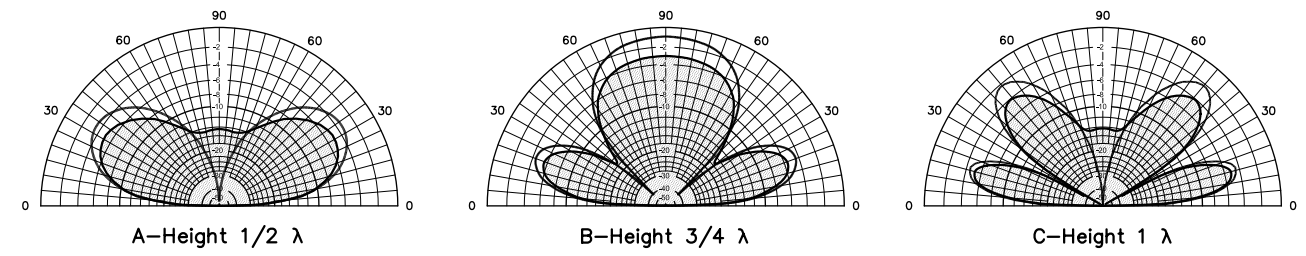

Fig 27—Vertical-plane radiation patterns of half-wave horizontal dipole antennas at 45° from the antenna wire over flat ground. The solid-line and shaded curves represent the same conditions as in Figs 25 and 26. These patterns are scaled so they may be compared directly with those of Figs 25 and 26.

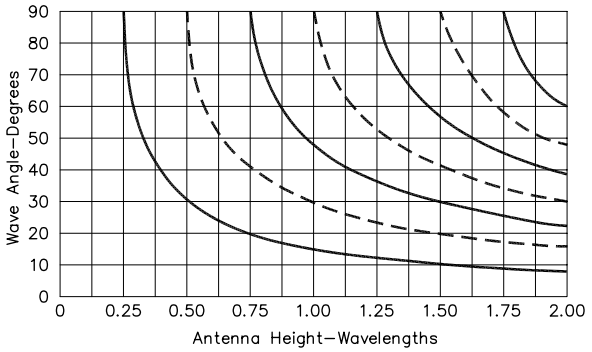

Fig 28—Angles at which nulls and maxima (factor = 6 dB) in the ground-reflection factor appear for antenna heights up to two wavelengths over flat ground. The solid lines are maxima, dashed lines nulls, for all horizontal antennas. See text for examples. Values may also be determined from the trigonometric relationship θ = arc sin (A/4h), where θ is the wave angle and h is the antenna height in wavelengths. For the first maximum, A has a value of 1; for the first null A has a value of 2, for the second maximum 3, for the second null 4, and so on.

communications to various target geographic locations of interest. Chapter 23, Radio Wave Propagation, and the CD-ROM in the back of this book give details about the range of angles required for target locations around the world. It is very useful to overlay plots of these angles together with the elevation pattern for horizontally polarized antennas at various heights above flat ground. This will be demonstrated in detail later in this chapter.

Vertically Polarized Antennas

In the case of a vertical λ/2 dipole or a ground-plane antenna, the horizontal directional pattern is simply a circle at any elevation angle (although the actual field strength will vary, at the different elevation angles, with the height above ground). Hence, one vertical pattern is sufficient to give complete information (for a given antenna height) about the antenna in any direction with respect to the wire. A series of such patterns for various heights is given in **Fig 29**. Rotating the plane pattern about the zenith axis of the graph forms the three-dimensional radiation pattern in each case.

The solid-line curves represent the radiation patterns of the λ/2 vertical dipole at different feed-point heights over perfectly conducting ground. The shaded curves in Fig 29 show the patterns produced by the same antennas at the same heights over average ground (G = 0.005 S/m, k = 13) at 14 MHz. The PBA in this case is 14.8°.

In short, far-field losses for vertically polarized antennas are highly dependent on the conductivity and dielectric constant of the earth around the antenna, extending far beyond the ends of any radials used to complete the ground return for the near field. Putting more radials out around the antenna may well decrease ground-return losses in the reactive near field for a vertical monopole, but will not increase radiation at low elevation launch angles in the far field, unless the radials can extend perhaps 100 wavelengths in all directions! Aside from moving to the fabled "salt water swamp on a high hill," there is very little that someone can do to change the character of the ground that affects the far-field pattern of a real vertical. Classical texts

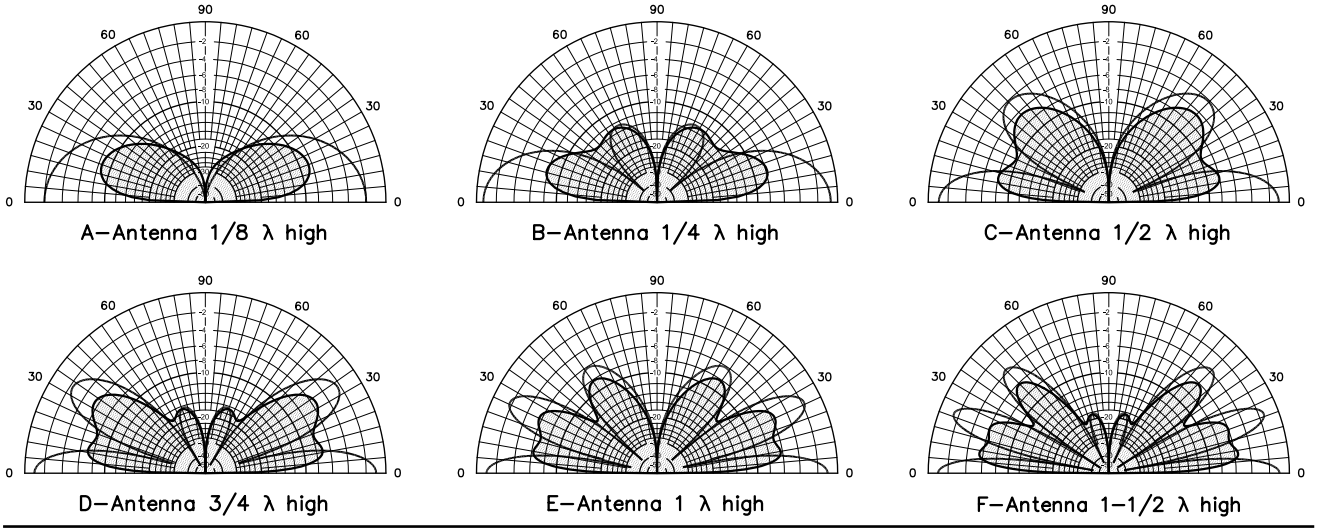

Fig 29—Vertical-plane radiation patterns of a ground-plane antenna above flat ground. The height is that of the ground plane, which consists of four radials in a horizontal plane. Solid lines are perfect-earth patterns; shaded curves show the effects of real earth. The patterns are scaled—that is, they may be directly compared to the solid-line ones for comparison of losses at any wave angle. These patterns were calculated for average ground (k = 13, G = 0.005 S/m) at 14 MHz. The PBA for these conditions is 14.8°. Add 6 dB to values shown for absolute gain in dBd over dipole in free space.

on verticals often show elevation patterns computed over an "infinitely wide, infinitely conducting ground plane." Real ground, with finite conductivity and less than perfect dielectric constant, can severely curtail the low-angle radiation at which verticals are supposed to excel.

While real verticals over real ground are not a surefire method to achieve low-angle radiation, cost versus performance and ease of installation are still attributes that can highly recommend verticals to knowledgeable builders. Practical installations for 160 and 80 meters rarely allow amateurs to put up horizontal antenna high enough to radiate effectively at low elevation angles. After all, a half-wave on 1.8 MHz is 273 feet high, and even at such a lofty height the peak radiation would be at a 30° elevation angle.

The Effects of Irregular Local Terrain in the Far Field

The following material is condensed and updated from an article by R. Dean Straw, N6BV, in July 1995 *QEX* magazine. *HFTA* (HF Terrain Assessment) and supporting data files are included on the CD-ROM at the back of this book. *HFTA* is the latest version of the *YT* program included with earlier editions of *The ARRL Antenna Book*.

Choosing a QTH for DXing

The subject of how to choose a QTH for working DX has fascinated hams since the beginning of amateur operations. No doubt, Marconi probably spent a lot of time wandering around Newfoundland looking for a great radio QTH before making the first transAtlantic transmission. Putting together a high-performance HF station for contesting or DXing has always followed some pretty simple rules. First, you need the perfect QTH, preferably on a rural mountaintop or at least on top of a hill. Even better yet, you need a mountaintop surrounded by seawater! Then, after you have found your dream QTH, you put up the biggest antennas you possibly can, on the highest towers you can afford. Then you work all sorts of DX—sunspots willing, of course.

The only trouble with this straightforward formula for success is that it doesn't always work. Hams fortunate enough to be located on mountain tops with really spectacular drop-offs often find that their highest antennas don't do very well, especially on 15 or 10 meters, but often even on 20 meters. When they compare their signals with nearby locals in the flatlands, they sometimes (but not always) come out on the losing end, especially when sunspot activity is high.

On the other hand, when the sunspots drop into the cellar, the high antennas on the mountaintop are usually the ones crunching the pileups—but again, not always. So, the really ambitious contest aficionados, the guys with lots of resources and infinite enthusiasm, have resorted to putting up antennas at all possible heights, on a multitude of towers.

There is a more scientific way to figure out where and how high to put your antennas to optimize your signal during all parts of the 11-year solar cycle. We advocate a *system approach* to HF station design, in which you need to know the following:

1. The range of elevation angles necessary to get from point A to point B
2. The elevation patterns for various types and configurations of antennas
3. The effect of local terrain on elevation patterns for horizontally polarized antennas.

WHAT IS THE RANGE OF ELEVATION ANGLES NEEDED?

Up until 1994, *The ARRL Antenna Book* contained only a limited amount of information about the elevation angles needed for communication throughout the world. In the 1974 edition, Table 1-1 in the Wave Propagation chapter was captioned: "Measured vertical angles of arrival of signals from England at receiving location in New Jersey."

What the caption didn't say was that Table 1-1 was derived from measurements made during 1934 by Bell Labs. The highest frequency data seemed pretty shaky, considering that 1934 was the low point of Cycle 17. Neither was this data applicable to any other path, other than the one from New Jersey to England. Nonetheless, many amateurs located throughout the US tried to use the sparse information in Table 1-1 as the only rational data they had for determining how high to mount their antennas. (If they lived on hills, they made estimates of the effect of the terrain, assuming that the hill was adequately represented by a long, unbroken slope. More on this later.)

In 1993 ARRL HQ embarked on a major project to tabulate the range of elevation angles from all regions of the US to important DX QTHs around the world. This was accomplished by running many thousands of computations using the *IONCAP* computer program. *IONCAP* has been under development for more than 25 years by various agencies of the US government and is considered the standard of comparison for propagation programs by many agencies, including the Voice of America, Radio Free Europe, and more than 100 foreign governments throughout the world. *IONCAP* is a real pain in the neck to use, but it is the standard of comparison.

The calculations were done for all levels of solar activity, for all months of the year, and for all 24 hours of the

day. The results were gathered into some very large databases, from which special custom-written software extracted detailed statistics. The results appeared in summary form in Tables 4 through 13 printed in Chapter 23, Radio Wave Propagation, of the 17th Edition and in more detail on the diskette included with that book. (This book, the 20th Edition, contains even more statistical data, for more areas of the world, on the accompanying CD-ROM.)

Fig 30 shows the full range of elevation angles (represented as vertical bars) for the 20-meter path from New England (centered on Newington, Connecticut) to all of Europe. This is for all openings, in all months, over the entire 11-year solar cycle. The most likely elevation angle occurs at 5° for about 13% of the times when the 20-meter band is open to Europe from New England. From 4° to 6° the band is open a total of about 34% of the times the band is open. There is a secondary peak between 10° to 12°, occurring for a total of about 25% of the times the band is open.

Overlaid on Fig 30 along with the elevation-angle statistics are the elevation-plane responses for three different horizontally polarized Yagi beams, all over flat ground. The first is mounted 140 feet high, 2 λ in terms of wavelength. The second Yagi is mounted 70 feet high (at 1 λ) and the third is 35 feet (0.5 λ). The 140-foot high antenna has a deep null at 15°, but it also has the highest response (13.4 dBi) of the three at the statistical peak elevation angle of 5°. However, at 12°—where the band is open some 9% of the time—the 140-foot high Yagi is down 4 dB compared to the 70-foot antenna.

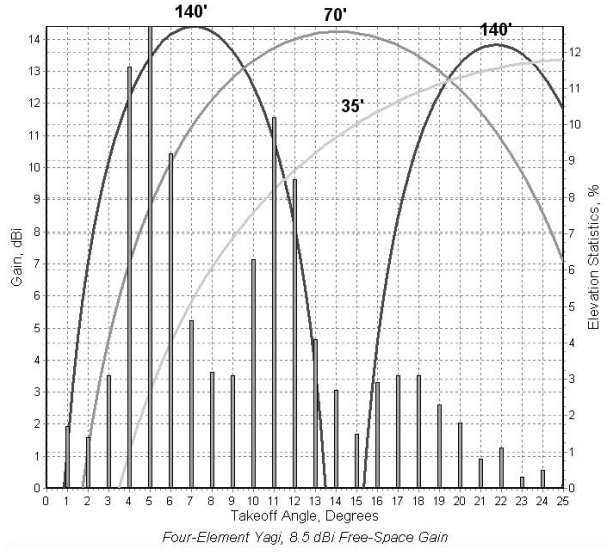

Fig 30—Graph showing 20-meter percentage of all openings from New England to Europe versus elevation angles, together with overlay of elevation patterns over flat ground for three 20-meter antenna systems. The most statistically likely angle at which the band will be open is 5°, although at any particular hour, day, month and year, the actual angle will likely be different. Note the deep null exhibited by the 140-foot high antenna centered at 14°.

The 70-foot high Yagi arguably covers the overall range best, since it has no disastrous nulls in the 1° to 25° range, where most of the action is occurring on 20 meters. At 5°, however, its response is only 8.8 dBi, 4.6 dB down from the 140-foot high antenna at that angle. The 35-foot antenna peaks above 26° in elevation angle, and is down some 10.4 dB compared to the 140-foot antenna at 5°. Obviously, no single antenna covers the complete range of elevation angles needed.

Note that the highest Yagi has a strong *second lobe* peaking at 22°. Let's say that you could select between two antennas, one at 140 and one at 70 feet, and that the incoming angle for a particular distant station is 22°. You might be fooled into thinking that the incoming angle is around 6°, favoring the first peak of the higher antenna, when in truth the angle is relatively high. The 70-foot antenna's response would be lower at 22° than the higher one, but only because the 140-foot antenna is operating on its second lobe. (What would clinch a determination of the correct incoming angle—6° or 22°—would be the response of the 35-foot high Yagi, which would be close to its peak at 22°, while it would be very far down at 6°.)

Now, we must emphasize that these elevation angles are *statistical entities*— in other words, just because 5° is the "statistically most likely angle" for the 20-meter path from New England to Europe doesn't mean that the band will be open at 11° at any particular hour, on a particular day, in a particular month, in any particular year. In fact, however, experience agrees with the *IONCAP* computations: the 20-meter path to Europe usually opens at a low angle in the New England morning hours, rising to about 11° during the afternoon, when the signals remain strongest throughout the afternoon until the evening in New England.

What would happen if we were to feed all three Yagi at 140, 70 and 35 feet in-phase as a stack? **Fig 31** shows this situation, along with a more highly optimized stack at 120, 80 and 40 feet that better covers the overall range of elevation angles from Connecticut to Europe.

Now see **Fig 32**, which uses the same 120/80/40-foot stack of 20-meter antennas as in Fig 31, but this time from Seattle, Washington, to Europe. For comparison, the response of a single 4-element Yagi at 100 feet over flat ground is also shown in Fig 32. Just because 5º is the statistically most prevalent angle (occurring some 13% of the time) from Seattle to Europe on 20 meters, this doesn't mean that the actual angle *at any particular moment in time* might not be 10º, or even 2º. The statistics for W7 to Europe say that 5º is the most likely angle, but 20-meter signals from Europe arrive at angles ranging from 1º to 18º. Note that this range of angles is quite a bit less than from W1 to Europe, which is much closer geographically to Europe than is the Pacific Northwest coast of the US. If you design an antenna system to cover all possible angles needed to talk to Europe from Seattle (or from Seattle to Europe) on 20 meters, you would need to cover the full range from 1º to 18º equally well.

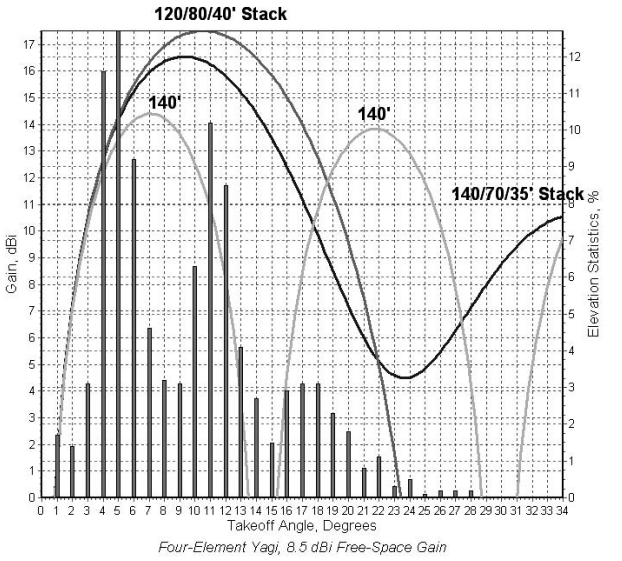

Fig 31—Graph showing results of stacking antennas at different heights on the same tower to cover a wider range of elevation angles, in this case for the path from Connecticut (W1) to all of Europe on 20 meters. The optimized stack at 120/80/40 feet covers the needed range of elevation angles better than the stack at 140/70/35 feet or the single Yagi at 140 feet.

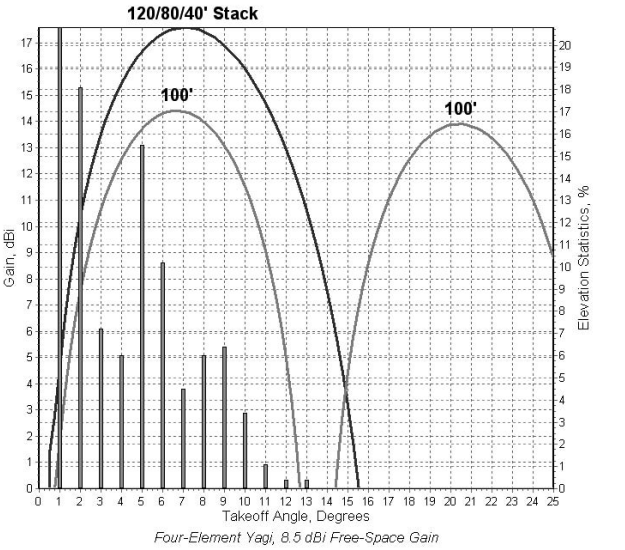

Fig 33—Graph showing 15-meter percentage of all openings from Chicago to Southern Africa, together with overlay of elevation patterns over flat ground for two 15-meter antenna systems. On this long-distance, low-angle path, higher antennas are again most effective.

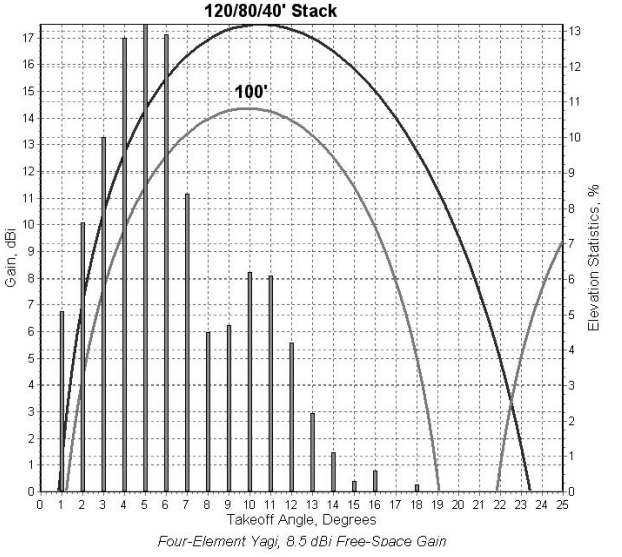

Fig 32—Graph showing 20-meter percentage of all openings, this time from Seattle, WA, to Europe, together with an overlay of elevation patterns over flat ground for two 20-meter antenna systems. The statistically most likely angle on this path is 5°, occurring about 13% of the time when the band is actually open. Higher antennas predominate on this low-angle path.

Similarly, if you wish to cover the full range of elevation angles from Chicago to Southern Africa on 15 meters, you would need to cover 1° to 13°, even though the most statistically likely signals arrive at 1°, for 21% of the time when that the band is open for that path. See **Fig 33**.

It is important to recognize that Figs 30 through 33 are for flat ground. When the antennas are mounted over irregular local terrain, things get much more complicated. First, however, we'll discuss general-purpose antenna modeling programs as they try to model real terrain.

DRAWBACKS OF COMPUTER MODELS FOR ANTENNAS OVER REAL TERRAIN

Modern general-purpose antenna modeling programs such as *NEC* or *MININEC* (or their commercially upgraded equivalents, such as *NEC-Win Plus*, *EZNEC* and *EZNEC ARRL*) can accurately model almost any type of antenna commonly used by radio amateurs. In addition, there are specialized programs specifically designed to model Yagis efficiently, such as *YO* or *YW* (Yagi for Windows, bundled on the CD-ROM with this book) or *YagiMax*. These programs however are all unable to model antennas accurately over anything other than *purely flat ground*.

While both *NEC* and *MININEC* can simulate irregular ground terrain, they do so in a decidedly crude manner, employing step-like concentric rings of height around an antenna. The documentation for *NEC* and *MININEC* both clearly state that diffraction off these steps is not modeled.

Common experience among serious modelers is that the warnings in the manuals are worth heeding.

Although you can analyze and even optimize antenna designs using free-space or flat-earth ground models, it is *diffraction* that makes the real world a very, very complicated place. This should be clarified—diffraction is hard, even tortuous, to analyze properly, but it makes analysis of real world results far more believable than a flat-world reflection model does.

RAY-TRACING OVER UNEVEN LOCAL TERRAIN

The Raytracing Technique

First, let's look at a simple raytracing procedure involving only horizontally polarized reflections, with no diffractions. From a specified height on the tower, an antenna shoots "rays" (just as though they were bullets) in 0.25° increments from +35° above the horizon to –35° below the horizon. Each ray is traced over the foreground terrain to see if it hits the ground at any point on its travels in the direction of interest. If it does hit the ground, the ray is reflected following the classical *law of reflection*. That is, the outgoing angle equals the incoming angle, reflected through the normal to the slope of the surface. Once the rays exit into the ionosphere, the individual contributions are vector-summed to create the overall far-field elevation pattern.

The next step in terrain modeling involves adding *diffractions* as well as reflections. At the Dayton antenna forum in 1994, Jim Breakall, WA3FET, gave a fascinating and tantalizing lecture on the effect of foreground terrain. Later Breakall, Dick Adler, K3CXZ, Joel Young and a group of other researchers published an extremely interesting paper entitled "The Modeling and Measurement of HF Antenna Skywave Radiation Patterns in Irregular Terrain" in July 1994 *IEEE Transactions on Antennas and Propagation*. They described in rather general terms the modifications they made to the *NEC-BSC* program. They showed how the addition of a ray-tracing reflection and diffraction model to the simplistic stair-stepped reflection model in regular *NEC* gave far more realistic results. For validation, they compared actual pattern measurements made on a site in Utah (with an overflying helicopter) to computed patterns made using the modified *NEC* software. However, because the US Navy funded this work the software remained for a long time a military secret.

Thumbnail History of the Uniform Theory of Diffraction

It is instructive to look briefly at the history of how *Geometric Optics* (GO) evolved (and still continues to evolve) into the *Uniform Theory of Diffraction* (UTD). The following is summarized from the historical overview in one book found to be particularly useful and comprehensive on the subject of UTD: *Introduction to the Uniform Geometrical Theory of Diffraction*, by McNamara, Pistorius, and Malherbe.

Many years before the time of Christ, the ancient Greeks studied optics. Euclid is credited with deriving the law of reflection about 300 BC. Other Greeks, such as Ptolemy, were also fascinated with optical phenomena. In the 1600s, a Dutchman named Snell finally figured out the law of refraction, resulting in *Snell's law*. By the early 1800s, the basic world of classical optics was pretty well described from a mathematic point of view, based on the work of a number of individuals.

As its name implies, classical geometric optical theory deals strictly with geometric shapes. Of course, the importance of geometry in optics shouldn't be minimized—after all, we wouldn't have eyeglasses without geometric optics. Mathematical analysis of shapes utilizes a methodology that traces the paths of straight-line *rays* of light. (Note that the paths of rays can also be likened to the straight-line paths of particles.) In classical geometric optics, however, there is no mention of three important quantities: phase, intensity and polarization. Indeed, without phase, intensity or polarization, there is no way to deal properly with the phenomenon of *interference*, or its cousin, *diffraction*. These phenomena require theories that deal with *waves* rather than rays.

Wave theory has also been around for a long time, although not as long as geometry. Workers like Hooke and Grimaldi had recorded their observations of interference and diffraction in the mid 1600s. Huygens had used elements of wave theory in the late 1600s to help explain refraction. By the late 1800s, the work of Lord Rayleigh, Sommerfeld, Fresnel, Maxwell and many others led to the full mathematic characterization of all electromagnetic phenomena, light included.

Unfortunately, ray theory doesn't work for many problems, at least ray theory in the classical optical form. The real world is a lot more jagged, pointy and fuzzy in shape than can be described in a totally rigorous mathematic fashion. Some properties of the real world are most easily explained on the micro level using electrons and protons as conceptual objects, while other macro phenomena (like resonance, for example) are more easily explained in terms of waves. To get a handle on a typical real-world physical situation, a combination of classical ray theory and wave theory was needed.

The breakthrough in the combination of classical geometric optics and wave concepts came from J. B. Keller of Bell Labs in 1953, although he published his work in the early 1960s. In the very simplest of terms, Keller introduced the notion that shooting a ray at a diffraction *wedge* causes wave interference at the tip, with an infinite number of diffracted waves emanating from the diffraction point. Each diffracted wave can be considered to be a point source radiator at the place of generation, the diffraction point. Thereafter, the paths of individual waves can be traced as

though they were individual classical optic rays again. What Keller came up with was a reasonable mathematical description of what happens at the tip of the diffraction wedge.

Fig 34 is a picture of a simple diffraction wedge, with an incoming ray launched at an angle of α_r, referenced to the horizon, impinging on it. The diffraction wedge here is considered to be perfectly conducting, and hence impenetrable by the ray. The wedge generates an infinite number of diffracted waves, going in all directions not blocked by the wedge itself. The amplitudes and phases of the diffracted waves are determined by the interaction at the wedge tip, and this in turn is governed by the various angles associated with the wedge. Shown in Fig 34 are the included angle a of the wedge, the angle ϕ' of the incoming ray (referenced to the incoming surface of the wedge), and the observed angle ϕ of one of the outgoing diffracted waves, also referenced to the wedge surface.

The so-called *shadow boundaries* are also shown in Fig 34. The Reflection-Shadow Boundary (RSB) is the angle beyond which no further reflections can take place for a given incoming angle. The Incident-Shadow Boundary (ISB) is that angle beyond which the wedge's face blocks any incident rays from illuminating the observation point.

Keller derived the amplitude and phase terms by comparing the classical Geometric Optics (GO) solution with the exact mathematical solution calculated by Sommerfeld for a particular case where the boundary conditions were well known—an infinitely long, perfectly conducting wedge illuminated by a plane wave. Simply speaking, whatever was left over had to be diffraction terms. Keller combined these diffraction terms with GO terms to yield the total field everywhere.

Keller's new theory became known as the *Geometric Theory of Diffraction* (abbreviated henceforth as GTD). The beauty of GTD was that in the regions where classical GO predicted zero fields, the GTD "filled in the blanks," so to speak. For example, see **Fig 35**, showing the terrain for a hypothetical case, where a 60-foot high 4-element 15-meter Yagi illuminates a wide, perfectly flat piece of ground. A 10-foot high rock has been placed 400 feet away from the tower base in the direction of outgoing rays. **Fig 36** shows the elevation pattern predicted using reflection-only GO techniques. Due to blockage of the direct wave (A) trying to shoot past the 10-foot high rock, and due to blockage of (B) reflections from the flat ground in front of the rock by the rock, there is a *hole* in the smooth elevation pattern.

Now, doesn't it defy common sense to imagine that a single 10-foot high rock will really have such an effect on a 15-meter signal? Keller's GTD took diffraction effects into account to show that waves do indeed sneak past and over the rock to fill in the pattern. The whole GTD scheme is very clever indeed.

However, GTD wasn't perfect. Keller's GTD predicts some big spikes in the pattern, even though the overall shape of the elevation pattern is much closer to reality than a simple GO reflection analysis would indicate. The region right at the RSB and ISB shadow boundaries is where problems are found. The GO terms go to zero at these points because of blockage by the wedge, while Keller's diffraction terms tend to go to infinity at these very spots. In mathematical terms this is referred to as a *caustic problem*. Nevertheless, despite these nasty problems at the ISB and RSB, the GTD provided a remarkably better solution to diffraction problems than did classical GO.

In the early 1970s, a group at Ohio State University under R. G. Kouyoumjian and P. H. Pathak did some pivotal work to resolve this caustic problem, introducing what amounts to a clever *fudge factor* to compensate for the tendency of the diffraction terms at the shadow boundaries to go to infinity. They introduced what is known as a *transition function*, using a form of Fresnel integral. Most importantly, the Ohio State researchers also created several FORTRAN computer programs to compute the amplitude and phase of diffraction components. Now computer hackers could get to work!

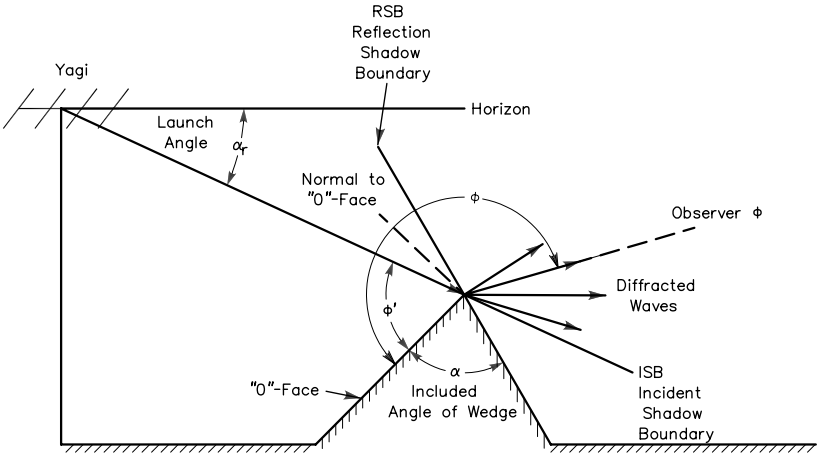

Fig 34—Diagram showing diffraction mechanism of ray launched at angle α_r below the horizon at a diffraction wedge, whose included angle is α. Referenced to the incident face (the *o-face* as it is called in UTD terminology), the incoming angle is ϕ' (phi prime). The wedge creates an infinite number of diffracted waves. Shown is one whose angle referenced to the o-face is ϕ, the so-called *observation angle* in UTD terminology.

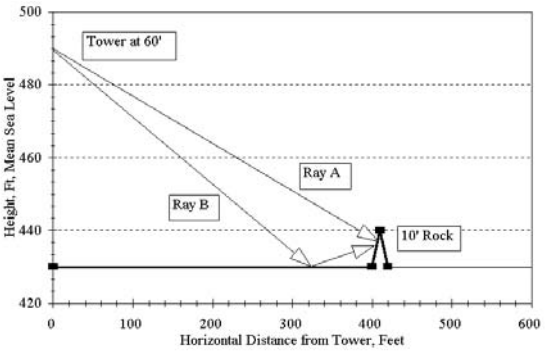

Fig 35—Hypothetical terrain exhibiting so-called "10-foot rock effect." The terrain is flat from the tower base out to 400 feet, where a 10-foot high rock is placed. Note that this forms a diffraction wedge, but that it also blocks direct waves trying to shoot through it to the flat surface beyond, as shown by Ray A. Ray B reflects off the flat surface before it reaches the 10-foot rock, but it is blocked by the rock from proceeding further. A simple Geometric Optics (GO) analysis of this terrain without taking diffraction into account will result in the elevation response shown in Fig 36.

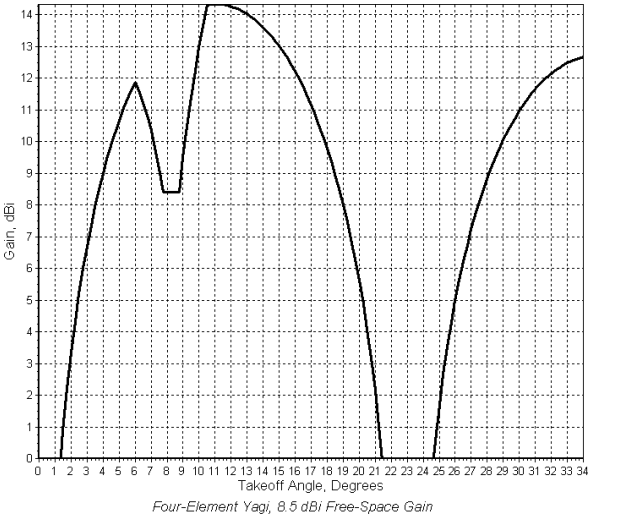

Fig 36—Elevation response for rays launched at terrain in Fig 35 from a height of 60 feet using a 4-element Yagi. This was computed using a simple Geometrical Optics (GO) reflection-only analysis. Note the *hole* in the response between 6° to 10° in elevation. It is not reasonable for a 10-foot high rock to create such a disturbance at 21 MHz!

The program that finally resulted is called *HFTA*, standing for "HF Terrain Assessment." (The DOS version of *HFTA* was known as *YT*, standing for "Yagi Terrain.") As the name suggests, *HFTA* analyzes the effect of local terrain on HF propagation through the ionosphere. It is designed for horizontally polarized Yagis, although it will model the effects of a simple flattop dipole also. The accurate appraisal of the effect of terrain on vertically polarized signals is a far more complex problem than for horizontally polarized waves, and *HFTA* doesn't do verticals.

SIMULATION OF REALITY—SOME SIMPLE EXAMPLES FIRST

We want to focus first on some simple results, to show that the computations do make some sense by presenting some simulations over simple terrains. We've already described the "10-foot rock at 400 feet" situation, and showed where a simple GO reflection analysis is inadequate to the task without taking diffraction effects into account.

Now look at the simple case shown in **Fig 37**, where a very long, continuous downslope from the tower base is shown. Note that the scales used for the X and Y axes are different: the Y-axis changes 300 feet in height (from 800 to 1100 feet), while the X-axis goes from 0 to 3000 feet. This exaggerates the apparent steepness of the downwards slope, which is actually a rather gentle slope, at $\tan^{-1}(1000 - 850) / (3000 - 0) = -2.86°$. In other words, the terrain falls 150 feet in height over a range of 3000 feet from the base of the tower.

Fig 38 shows the computed elevation response for this terrain profile, for a 4-element horizontally polarized Yagi on a 60-foot tower. The response is compared to that of an identical Yagi placed 60 feet above flat ground. Compared to the "flatland" antenna, the hilltop antenna has an elevation response shifted over by almost 3° towards the lower elevation angles. In fact, this shift is directly due to the –2.86° slope of the hill. Reflections off the slope are tilted by the slope. In this situation there is a single diffraction at the bottom of the gentle slope at 3000 feet, where the program assumes that the terrain becomes flat.

Look at **Fig 39**, which shows another simple terrain profile, called a "Hill-Valley" scenario. Here, the 60-foot high tower stands on the edge of a gentle hill overlooking a long valley. Once again the slope of the hill is exaggerated by the different X and Y-axes. **Fig 40** shows the computed elevation response at 21.2 MHz for a 4-element Yagi on a 60-foot high tower at the edge of the slope.

Once again, the pattern is overlaid with that of an identical 60-foot-high Yagi over flat ground. Compared to the flatland antenna, the hilltop antenna's response above 9° in elevation is shifted by almost 3° towards the lower elevation angles. Again, this is due to reflections off the downward slope. From 1° to 9°, the hilltop pattern is enhanced even more compared to the flatland antenna, this time by diffraction occurring at the bottom of the hill.

Now let's see what happens when there is a hill ahead in the direction of interest. **Fig 41** depicts such a situation, labeled "Hill-Ahead." Here, at a height of 400 feet above mean sea level, the land is flat in front of the tower, out to a distance 500 feet, where the hill begins. The hill then rises 100 feet over the range 500 to 1000 feet away

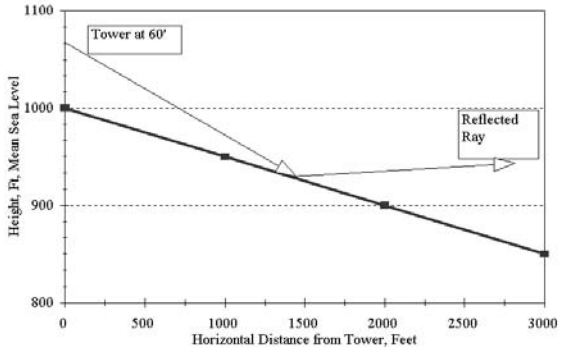

Fig 37—A long, gentle downwards-sloping terrain. This terrain has no explicit diffraction points and can be analyzed using simple GO reflection techniques.

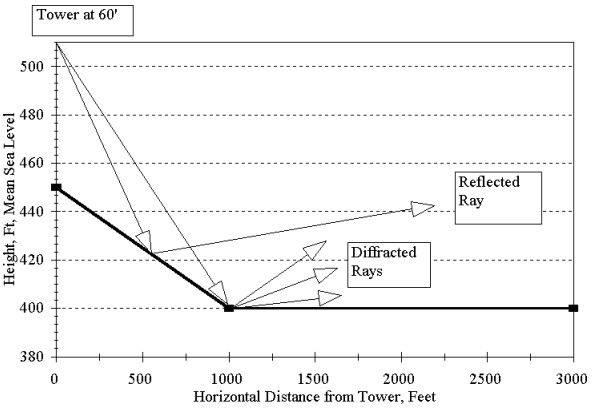

Fig 39—"Hill-Valley" terrain, with reflected and diffracted rays.

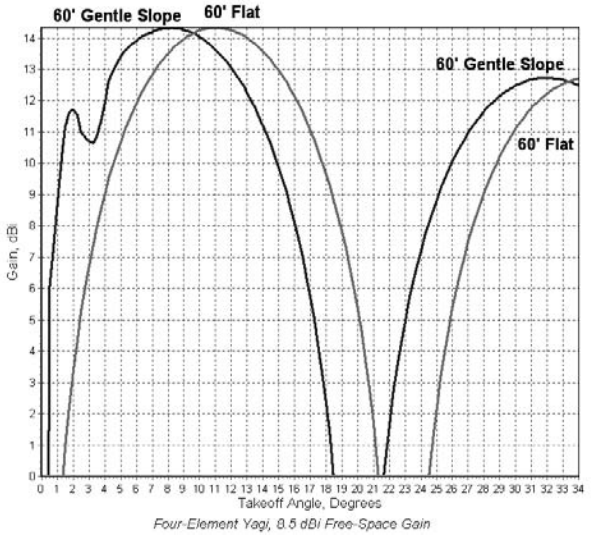

Fig 38—Elevation response for terrain shown in Fig 37, using a 4-element 15-meter Yagi, 60-foot high. Note that the shape of the response is essentially shifted towards the left, towards lower elevation angles, by the angle of the sloping ground. For reference, the response for an identical Yagi placed over flat ground is also shown.

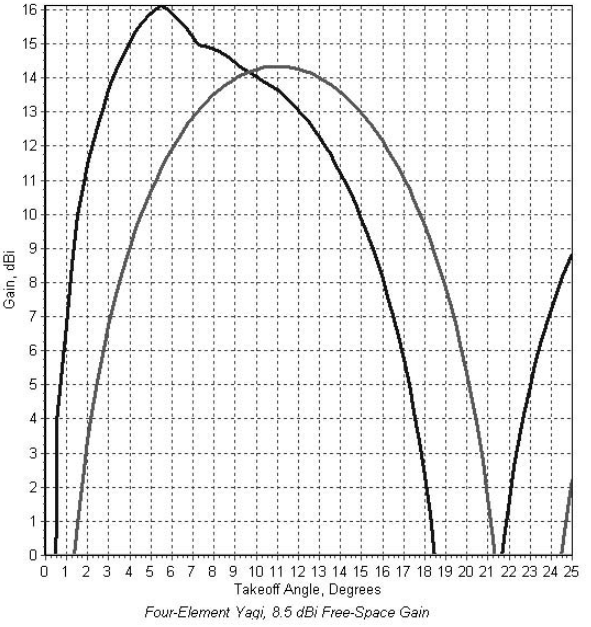

Fig 40—Elevation response computed by *HFTA* program for single 4-element 15-meter Yagi at 60 feet above "Hill-Valley" terrain shown in Fig 39. Note that the slope has caused the response in general to be shifted towards lower elevation angles. At 5° elevation, the diffraction components add up to increase the gain slightly above the amount a GO-only analysis would indicate.

from the tower base. After that, the terrain is a plateau, at a constant 500 feet elevation.

Fig 42 shows the computed elevation pattern for a 4-element 21-MHz Yagi 60-feet high on the tower, compared again with an overlay for an identical 60-foot high antenna over flat ground. The hill blocks low-angle waves directly radiated from the antenna from 0° to 2.3°. In addition, waves that would normally be reflected from the ground, and that would normally add in phase from about 2.3° to 12°, are blocked by the hill also. Thus the signal at 8° is down almost 5 dB from the signal over flat ground, all due to the effect of the hill. Diffracted waves start kicking in once the direct wave rises enough above the horizon to illuminate the top edge of the hill. These diffracted waves tend to augment elevation angles above about 12°, which reflected waves can't reach.

Is there is any hope for someone in such a lousy QTH for DXing? **Fig 43** shows the elevation response for a truly heroic solution. This involves a stack of four 4element Yagis, mounted at 120, 90, 60 and 30 feet on the tower. Now, the total gain at low angles is just about comparable to that from a single 4-element Yagi mounted over flat ground. Where there's a ham, there is a way!

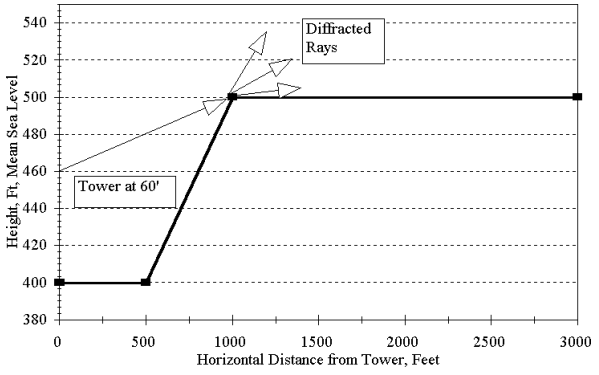

Fig 41—"Hill-Ahead" terrain, shown with diffracted rays created by illumination of the edge of the plateau at the top of the hill.

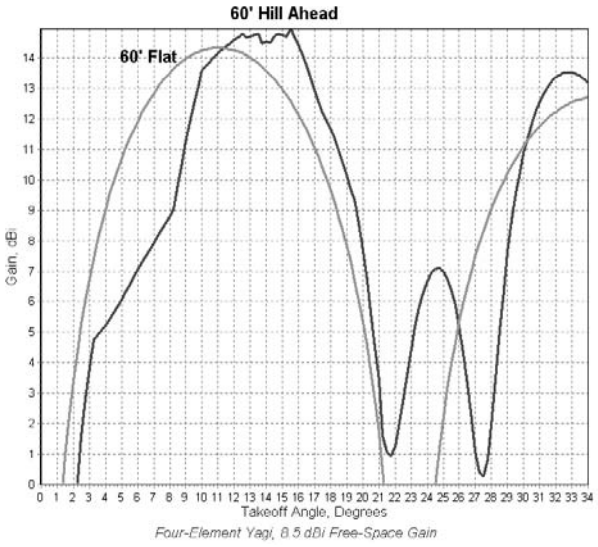

Fig 42—Elevation response computed by *HFTA* for "Hill-Ahead" terrain shown in Fig 41. Now the hill blocks direct rays and also precludes possibility of any constructive reflections. Above 10°, diffraction components add up together with direct rays to create the response shown.

At 5° elevation, four diffraction components add up (there are zero reflection components) to achieve the far-field pattern. This seems reasonable, because each of the four antennas is illuminating the diffraction point separately and we know that none of the four antennas can *see over* the hill directly to produce a reflection at a low launch angle.

At an elevation angle of 5°, 15-meter signals arrive from Europe from New England about 13% of the total time when the band is actually open. We can look at this another way. For about two-thirds of the times when the band is open on this path, the incoming angle is between 3° to 12°. For about one-third of the time, signals arrive above 10°, where the "heroic" four-stack is really beginning to come into its own.

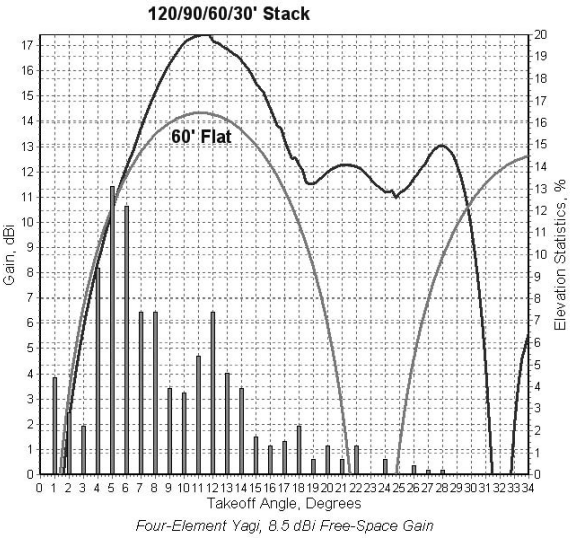

Fig 43—Elevation response of "heroic effort" to surmount the difficulties imposed by hill in Fig 41. This effort involves a stack of four 4-element Yagis in a stack starting at 120 feet and spaced at 30-foot increments on the tower. The response is roughly equivalent to a single 4-element Yagi at 60 feet above flat ground, hence the characterization as being a "heroic effort." The elevation-angle statistics from New England to Europe are overlaid on the graph for reference.

A More Complex Terrain

The results for simple terrains look reasonable; let's try a more complicated real-world situation. **Fig 44** shows the terrain from the New Hampshire N6BV/1 QTH towards Japan. The terrain was complex, with 52 different points *HFTA* identifies as diffraction points. **Fig 45** shows a labeled *HFTA* output for three different types of antennas on 20 meters: a stack at 120 and 60 feet, the 120-foot antenna by itself, and then a 120/60-foot stack over flat ground, for reference. The elevation-angle statistics for New England to Japan are overlaid on the graph also, making for a very complicated looking picture—it is a *lot* easier to decipher the lines on the color CRT, by the way than on a black-and-white printer.

Comparison of the same 120/60-foot stacks over irregular terrain and flat ground is useful to show where the terrain itself is affecting the elevation response. The flatland stack has more gain in the region of 3° to 7° than the same stack over the N6BV/1 local terrain towards Japan. On the other hand, the N6BV/1 local terrain boosts signals in the range of 8° to about 12°. This demonstrates the conservation of energy—you may gain a stronger signal at certain elevation angles, but you will lose gain at others. In this case, the N6BV/1 station always felt "weak" towards Japan on 20 meters, because the dominant angles are low.

Examination of the detailed data output from *HFTA* shows that at an elevation angle of 5°, there are 6159

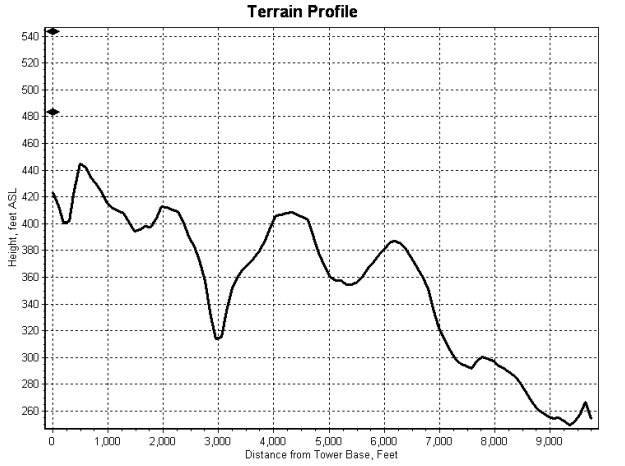

Fig 44—Terrain of N6BV in Windham, NH, towards Japan. *HFTA* identifies 52 different points where diffraction can occur.

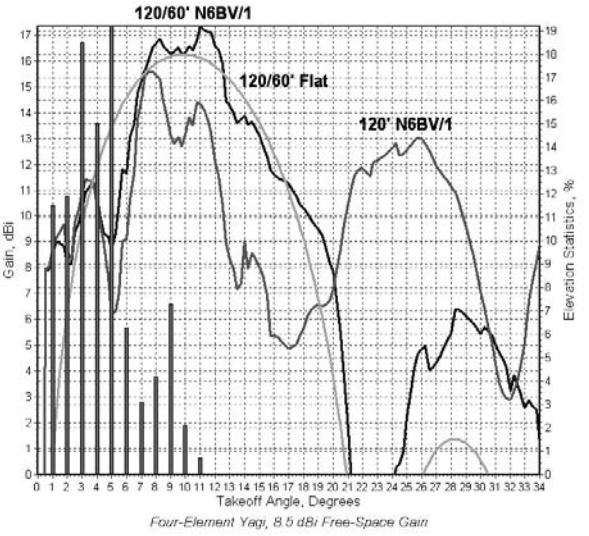

Fig 45—Elevation responses computed by *HFTA* for N6BV/1 terrain shown in Fig 44, for a stack of two 4-element 20-meter Yagis at 120 and 60 feet, together with the response for a single Yagi at 120 feet and a 120/60-foot stack over flat ground for reference. The response due to many diffraction and reflection components is quite complicated!

diffraction components. There are many, many signals bouncing around off the terrain on their trip to Japan! Note that because of blockage of some parts of the terrain, the 60-foot high Yagi cannot illuminate all the diffraction points, while the higher 120-foot Yagi is able to see these diffraction points.

It is fascinating to reflect on the thought that received signals coming down from the ionosphere to the receiver are having encounters with the terrain, but from the opposite direction. It's not surprising, given these kinds of interactions, that transmitting and receiving might not be totally reciprocal.

The 120/60-foot stack in Fig 45 achieves its peak gain of 17.3 dBi at 11° elevation, where it is about 3 dB stronger than the single Yagi at 120 feet. It maintains this 3-dB advantage over most of the range of incoming signals from Japan. This difference in performance between the stack and each antenna by itself was observed many times on the air. Much of the time when comparisons are being made, however, the small differences in signal are difficult to measure meaningfully, especially when the QSB varies signals by 20 dB or so during a typical QSO. It should be noted that the stack usually exhibited less fading compared to each antenna by itself.

USING *HFTA*

Manually Generating a Terrain Profile

The *HFTA* program uses two distinct algorithms to generate the far-field elevation pattern. The first is a simple reflection-only Geometric Optics (GO) algorithm. The second is the diffraction algorithm using the Uniform Theory of Diffraction (UTD). These algorithms work with a digitized representation of the terrain profile for a single azimuthal direction—for example, towards Japan or towards Europe.

You can generate a terrain file manually using a topographic map and a ruler or a pair of dividers. The HFTA.PDF file (accessed by clicking on the **Help** button) and on the accompanying CD-ROM gives complete instructions on how to create a terrain file manually (or automatically). The manual process is simple enough in concept. Mark on your US Geological Survey 7.5-minute map the exact location of your tower. You will find 7.5-minute maps available from some local sources, such as large hardware stores, but the main contact point is the U.S. Geological Survey, Denver, CO 80225 or Reston, VA 22092. Call 1-800-MAPS-USA. Ask for the folder describing the topographic maps available for your geographic area. Many countries outside the USA have topographic charts also. Most are calibrated in meters. To use these with *HFTA*, you will have to convert meters to feet by multiplying meters by 3.28 or else inserting a single line at the very beginning of the disk file, saying "meters" for *HFTA* to recognize meters automatically.

Mark off a pencil line from the tower base, in the azimuthal direction of interest, perhaps 45° from New England to Europe, or 335° to Japan. Then measure the distance from the tower base to each height contour crossed by the pencil line. Enter the data at each distance/height into an ASCII computer file, whose filename extension is "PRO," standing for *profile*.

Fig 46 shows a portion of the USGS paper map for the N6BV QTH in Windham, NH, along with lines scribed in several directions towards various parts of Europe and the Far East. Note that the elevation heights of the intermediate

contour lines are labeled manually in pencil in order to make sense of things. It is very easy to get confused unless you do this!

The terrain model used by *HFTA* assumes that the terrain is represented by flat *plates* connecting the elevation points in the *.PRO file with straight lines. The model is two dimensional, meaning that range and elevation are the only data for a particular azimuth. In effect, *HFTA* assumes that the width of a terrain plate is wide relative to its length. Obviously, the world is three-dimensional. If your shot in a particular direction involves aiming your Yagi down a canyon with steep walls, then it's pretty likely that your actual elevation pattern will be different than what *HFTA* tells you. The signals must careen horizontally from wall to wall, in addition to being affected by the height changes of the terrain. *HFTA* isn't designed to do canyons.

To get a true 3-D picture of the full effects of terrain, a terrain model would have to show azimuth, along with range and elevation, point-by-point for about two miles in every direction around the base of the tower. After you go through the pain of creating a profile for a single azimuth, you'll appreciate the immensity of the process if you were you try to create a full 360° 3D profile manually.

Terrain Data from the Internet

At one time digitized terrain data commonly available from the Internet didn't have sufficient resolution to be accurate enough for *HFTA*. Nowadays, the complete, accurate set of USGS topographic 7.5-minute maps are available at no cost on the Internet. You can use a program called *MicroDEM*, written by Professor Peter Guth at the US Naval Academy, to quickly and easily produce terrain data files suitable for *HFTA* from topographic data files. Dr Guth and the US Naval Academy have graciously allowed ARRL to include the *MicroDEM* program on the CD-ROM accompanying this book. It should be noted that besides automatically creating terrain profiles for *HFTA*, *MicroDEM* is a full-featured mapping program on its own.

Instructions for using *MicroDEM* are in the Help file for *HFTA* (HFTA.PDF), which you can access from the *HFTA* main window by clicking on the **Help** button. **Fig 47** shows a screen capture of the *MicroDEM* program for the N6BV/1 location in New Hampshire for an azimuth of 45° into Europe. The black/white rendering of the screen capture doesn't do justice to the same information in color. The computed terrain profile is plotted in the window at the right of Fig 47 and the data file is shown in the inset window at the top right.

Using *MicroDEM* and on-line USGS topographic map data, you can also automatically create up to 360 terrain profiles with 1° spacing of azimuths in a few seconds. (Specifying a 1° spacing is really overkill; most operator choose to create 72 profiles with 5° spacing.) On a topographic DEM (digital elevation model) map that covers the geographic

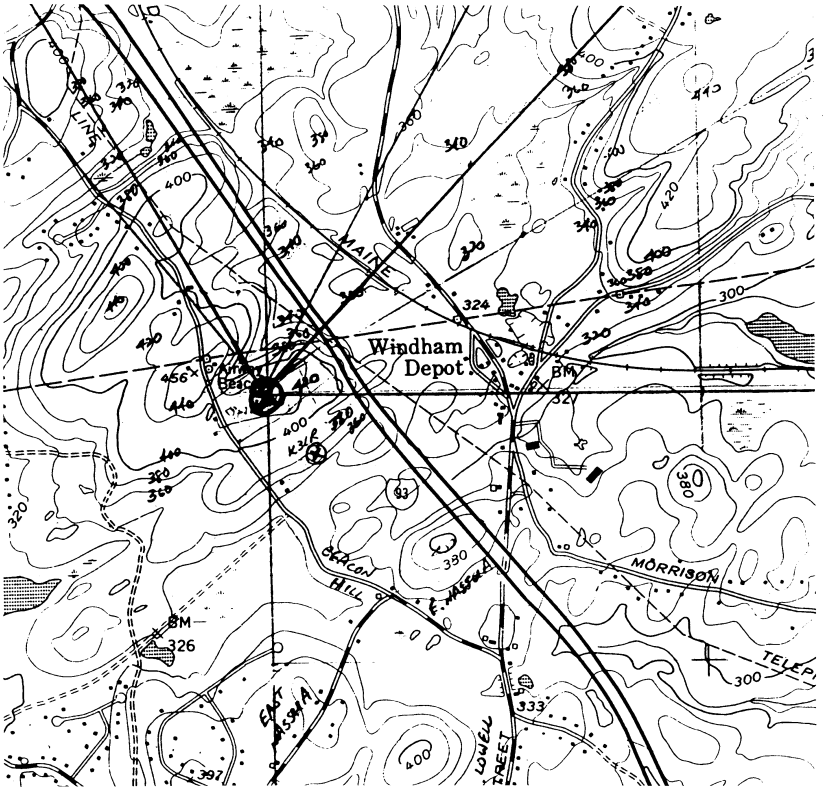

Fig 46—A portion of USGS 7.5 minute topographic map, showing N6BV/1 QTH, together with marks in direction of Europe and Japan from tower base. Note that the elevations contours were marked by hand to help eliminate confusion. This required a magnifying glass and a steady hand!

area of interest, you simply specify the latitude and longitude of a tower's location—found using a GPS receiver—and then ask *MicroDEM* for a **Viewshed**. See the *HFTA* **Help** file for the details.

Compare this automated several-second *MicroDEM* process to creating manual profiles on a paper topographic map—It can take up to an hour of meticulous measurements to manually create a single terrain profile!

Algorithm for Ray-Tracing the Terrain

Once a terrain profile is created, there are a number of mechanisms that *HFTA* takes into account as a ray travels over that terrain:

1. Classical ray reflection, with Fresnel ground coefficients.
2. Direct diffraction, where a diffraction point is illuminated directly by an antenna, with no intervening terrain features blocking the direct illumination.
3. When a diffracted ray is subsequently reflected off the terrain.
4. When a reflected ray encounters a diffraction point and causes another series of diffracted rays to be generated.
5. When a diffracted ray hits another diffraction point, generating another whole series of diffractions.

Certain unusual, bowl-shaped terrain profiles, with sheer vertical faces, can conceivably cause signals to reflect or diffract in a backwards direction, only to be reflected back again in the forward direction by the sheer-walled terrain to the rear. *HFTA* does not accommodate these interactions, mainly because to do so would increase the computation time too much. It only evaluates terrain in the forward direction along one azimuth of interest.

Fig 48 shows a portion of an *HFTA* screen capture in the direction towards Europe from the N6BV/1 location in New Hampshire on 21.2 MHz. It compares the results for a 90/60/30-foot stack of TH7DX tribanders to the same stack over flat land, and to a single antenna at 70 feet over flat ground. The 70-foot single antenna represents a pretty typical station on 15 meters. The terrain produces excellent gain at lower elevation angles compared to the same stack over flat ground. The stack is very close to or superior to the single 70-foot high Yagi at all useful elevation angles. Terrain can indeed exhibit a profound effect on the launch of signals into the ionosphere—for good or for bad.

HFTA's Internal Antenna Model

The operator selects the antenna used inside *HFTA* to be anything from a dipole to an 8-element Yagi. The default assumes a simple cosine-squared mathematic response, equivalent to a 4-element Yagi in free space. *HFTA* traces rays only in the forward direction from the tower along the azimuth of interest. This keeps the algorithms reasonably simple and saves computing time.

HFTA considers each antenna in a stack as a separate *point source*. The simulation begins to fall apart if a traveling wave type of antenna like a rhombic is used, particularly if the terrain changes under the antenna—that is, the ground is not flat under the entire antenna. For a typical Yagi, even a long-boom one, the point-source assumption is reasonable. The internal antenna model also assumes that the Yagi is horizontally polarized. *HFTA* does not do vertically polarized antennas, as discussed previously. The documentation for *HFTA* also cautions the user to work with practical spacings between stacked Yagis—0.5 λ or more

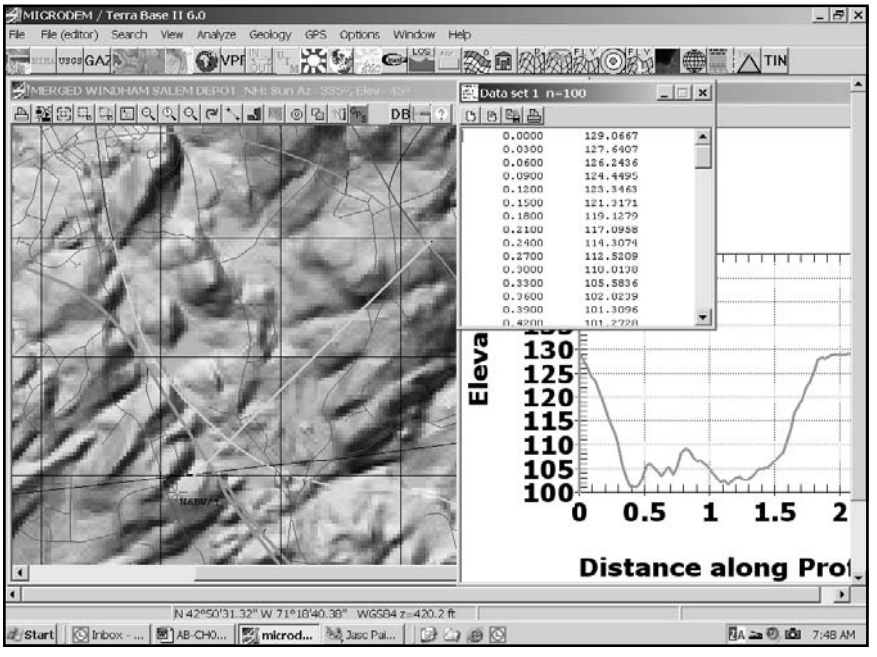

Fig 47—A screen-capture of the *MicroDEM* program, showing the topographic map for the same terrain shown in Fig 46, together with the computed terrain profile along an azimuth of 45° on the path towards Europe from the N6BV/1 location in Windham, NH.

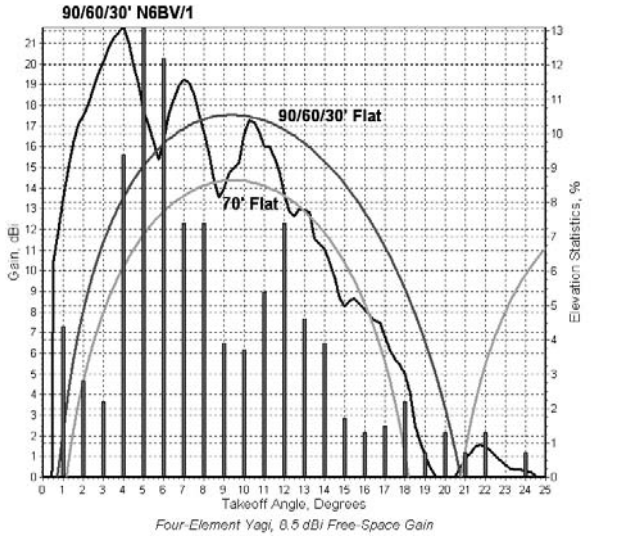

Fig 48—The 21-MHz elevation response for a stack of three TH7DX Yagis mounted on a single tower at 90/60/30 feet, at the N6BV/1 QTH for a 45° azimuth towards Europe. The terrain focuses the energy at low elevation angles compared to the same stack over flat ground. This illustrates once again the conservation of energy—Energy squeezed down into low elevation angles is stolen from other, higher, angles.

because *HFTA* doesn't explicitly model mutual coupling between Yagis in a stack.

HFTA compares well with the measurements for the horizontal antennas described earlier by Jim Breakall, WA3FET, using a helicopter in Utah. Breakall's measurements were done with a 15-foot high horizontal dipole.

More Details About *HFTA*

Frequency Coverage

HFTA can be used on frequencies higher than the HF bands, although the graphical resolution is only 0.25°. The patterns above about 100 MHz thus look rather grainy. The UTD is a *high-frequency-asymptotic* solution, so in theory the results become more realistic as the frequency is raised. Keep in mind too that *HFTA* is designed to model launch angles for skywave propagation modes, including E- and F-layer, and even Sporadic-E. Since by definition the ionospheric launch angles include only those above the horizon, direct line-of-sight UHF modes involving negative launch angles are not considered in *HFTA*.

See the HFTA.PDF documentation file for further details on the operation of *HFTA*. This file, as well as sample terrain profiles for some *big-gun* stations, is located on the CD-ROM accompanying this book.

BIBLIOGRAPHY

Source material and more extended discussion of the topics covered in this chapter can be found in the references listed below and in the textbooks listed at the end of Chapter 2, Antenna Fundamentals.

B. Boothe, "The Minooka Special," *QST*, Dec 1974.

Brown, Lewis and Epstein, "Ground Systems as a Factor in Antenna Efficiency," *Proc. IRE* , Jun 1937.

G. Brown, "The Phase And Magnitude Of Earth Currents Near Radio Transmitting Antennas," *Proc. IRE*, Feb 1935, pp 168-182.

R. Collin and F. Zucker, *Antenna Theory*, Chap 23 by J. Wait, Inter-University Electronics Series (New York: McGraw-Hill, 1969), Vol 7, pp 414-424.

T. Hullick, W9QQ, "A Two-Element Vertical Parasitic Array For 75 Meters," *QST*, Dec 1995, pp 38-41.

R. Jones, "A 7-MHz Vertical Parasitic Array," *QST*, Nov 1973.

T. Larsen, "The E-Field and H-Field Losses Around Antennas With a Radial Ground Wire System," *Journal of Research of the National Bureau of Standards*, D. Radio Propagation, Vol 66D, No. 2, Mar-Apr 1962, pp 189-204.

D. A. McNamara, C. W. I. Pistorius, J. A. G. Malherbe, *Introduction to the Geometrical Theory of Diffraction* (Norwood, MA: Artech House, 1994).

C. J. Michaels, "Some Reflections on Vertical Antennas," *QST*, Jul 1987.

C. J. Michaels, "Horizontal Antennas and the Compound Reflection Coefficient," *The ARRL Antenna Compendium, Vol 3* (Newington: ARRL, 1992).

R. Severns, N6LF, "Verticals, Ground Systems and Some History," *QST*, Jul 2000, pp 38-44.

J. Sevick, "The Ground-Image Vertical Antenna," *QST*, Jul 1971.

J. Sevick, "The W2FMI 20-Meter Vertical Beam," *QST*, Jun 1972.

J. Sevick, "The W2FMI Ground-Mounted Short Vertical," *QST*, Mar 1973.

J. Sevick, "A High Performance 20-, 40- and 80-Meter Vertical System," *QST*, Dec 1973.

J. Sevick, "The Constant-Impedance Trap Vertical," *QST*, Mar 1974.

J. Stanley, "Optimum Ground Systems for Vertical Antennas," *QST*, Dec 1976.

F. E. Terman, *Radio Engineers' Handbook*, 1st ed. (New York, London: McGraw-Hill Book Co, 1943).

Radio Broadcast Ground Systems, available from Smith Electronics, Inc, 8200 Snowville Rd, Cleveland, OH 44141.

The last major study that appeared in the Amateur literature on the subject of local terrain as it affects DX appeared in four *QST* "How's DX" columns, by Clarke Greene, K1JX, from October 1980 to January 1981. Greene's work was an update of a landmark Sep 1966 *QST* article entitled "Station Design for DX," by Paul Rockwell, W3AFM. The long-range profiles of several prominent, indeed legendary, stations in Rockwell's article are fascinating: W3CRA, W4KFC and W6AM.